Unique contribution of enhancer-driven and master-regulator genes to autoimmune disease revealed using functionally informed SNP-to-gene linking strategies

Kushal K. Dey[1], Steven Gazal[1], Bryce van de Geijn [1,3], Samuel Sungil Kim [1,4], Joseph Nasser[5], Jesse M. Engreitz[5], Alkes L. Price [1,2,5]

1 Department of Epidemiology, Harvard T. H. Chan School of Public Health, Boston, MA, USA
2 Department of Biostatistics, Harvard T.H. Chan School of Public Health, Boston, MA
3 Genentech, South San Francisco, CA
4 Department of Electrical Engineering and Computer Science, Massachusetts Institute of Technology, Cambridge, MA
5 Broad Institute of MIT and Harvard, Cambridge, MA, USA

Abstract

Gene regulation is known to play a fundamental role in human disease, but mechanisms of regulation vary greatly across genes. Here, we explore the contributions to disease of two types of genes: genes whose regulation is driven by enhancer regions as opposed to promoter regions (Enhancer-driven) and genes that regulate many other genes in trans (Master-regulator). We link these genes to SNPs using a comprehensive set of SNP-to-gene (S2G) strategies and apply stratified LD score regression to the resulting SNP annotations to draw three main conclusions about 11 autoimmune diseases and blood cell traits (average N=306K). First, Enhancer-driven genes defined in blood using functional genomics data (e.g. ATAC-seq, RNA-seq, PC-HiC) are uniquely informative for autoimmune disease heritability, after conditioning on a broad set of regulatory annotations from the baseline-LD model. Second, Master-regulator genes defined using trans-eQTL in blood are also uniquely informative for autoimmune disease heritability. Third, integrating Enhancer-driven and Master-regulator gene sets with protein-protein interaction (PPI) network information magnified their unique disease signal. The resulting PPI-enhancer gene score produced >2x stronger conditional signal (maximum standardized SNP annotation effect size ($\tau^\star$) = 2.0 (s.e. 0.3) vs. 0.91 (s.e. 0.21)), and >2x stronger gene-level enrichment for approved autoimmune disease drug targets (5.3x vs. 2.1x), as compared to the recently proposed Enhancer Domain Score (EDS). In each case, using functionally informed S2G strategies to link genes to SNPs that may regulate them produced much stronger disease signals (4.1x-13x larger $\tau^\star$ values) than conventional window-based S2G strategies. We conclude that Enhancer-driven and Master-regulator genes are uniquely informative for human disease, and that PPI networks and S2G strategies magnify these signals.

1 Introduction

Disease risk variants associated with complex traits and diseases predominantly lie in non-coding regulatory regions of the genes, motivating the need to assess the relative importance of genes for disease through the lens of gene regulation[1–6]. Several recent studies have performed disease-specific gene-level prioritization by integrating GWAS summary statistics data with functional genomics data, including gene expression and gene networks[7–14]. Here, we investigate the contribution to autoimmune disease of gene sets reflecting two specific aspects of gene regulation in blood—genes with strong evidence of enhancer-driven regulation (Enhancer-driven) and genes that regulate many other genes (Master-regulator); previous studies suggest that both of these characterizations are important for understanding human disease[9,15–25]. We further investigate whether integrate information from protein-protein interaction (PPI) networks[26,27] can magnify disease signals[10–12,28–32].

A major challenge in gene-level analyses of disease is to link genes to SNPs that may regulate them, a prerequisite to integrative analyses of GWAS summary statistics. Previous studies have often employed window-based strategies, linking each gene to all SNPs within a specific genomic distance; however, this approach lacks specificity. Here, we incorporated functionally informed SNP-to-gene (S2G) linking strategies that capture both distal and proximal components of gene regulation. We evaluated the resulting SNP annotations by applying stratified LD score regression[33] (S-LDSC) conditional on a broad set of coding, conserved, regulatory and LD-related annotations from the baseline-LD model[34,35], meta-analyzing the results across 11 autoimmune diseases and blood-related traits. We also assessed gene-level enrichment for disease-related gene sets, including approved drug targets for autoimmune disease[10].

Results

Background

We define an *annotation* as an assignment of a numeric value to each SNP with minor allele count $\geq$5 in a 1000 Genomes Project European reference panel[36], as in our previous work[33]; we primarily focus on annotations with values between 0 and 1. We define a *gene score* as an assignment of a numeric value between 0 and 1 to each gene; we primarily focus on binary gene sets defined by the top 10% of genes. We consider 11 gene scores prioritizing master-regulator genes, enhancer-driven genes, and genes with high network connectivity to enhancer-driven genes (Table 1). We define a *SNP-to-gene (S2G) linking strategy* as an assignment of 0, 1 or more linked genes to each SNP. We consider 10 S2G strategies capturing both distal and proximal gene regulation (see Methods, Figure 1A and Table 2). For each gene score X and S2G strategy Y, we define a corresponding *combined* annotation X $\times$ Y by assigning to each SNP the maximum gene score among genes linked to that SNP (or 0 for SNPs with no linked genes); this generalizes the standard approach of constructing annotations from gene scores using window-based strategies[8,9]. In particular, for each S2G strategy, we define a corresponding binary S2G annotation defined by SNPs linked to the set of all genes. We have publicly released all gene scores, S2G links, and annotations analyzed in this study (see URLs).

First, we employ gradient boosting[37] to integrate deep learning annotations with

(off-chromosome) fine-mapped SNPs for blood-related traits from previous studies[?,38,39] to generate boosted annotations representing an optimal combination of deep-learning annotations across features. Second, we improve the specificity of these annotations by restricting them to SNPs linked to genes using 10 (proximal and distal) SNP-to-gene (S2G) strategies[?] (Table 2). Third, we predict gene expression (and derive allelic-effect annotations) from (off-chromosome) deep learning annotations at SNPs implicated by S2G linking strategies—generalizing the previously proposed ExPecto approach[7], which incorporates deep learning annotations based on distance to TSS.

We assessed the informativeness of the resulting annotations for disease heritability by applying stratified LD score regression (S-LDSC)[33] to 11 independent blood-related traits (5 autoimmune diseases and 6 blood cell traits; average N=306K, Table S1) and meta-analyzing S-LDSC results across traits; we restricted our analyses to blood-related traits due to our focus on functional data in blood. We conditioned all analyses on a "baseline-LD-deep model" defined by 86 coding, conserved, regulatory and LD-related annotations from the baseline-LD model (v2.1)[34,35] and 14 additional jointly significant annotations from ref.[40]: 1 non-tissue-specific allelic-effect Basenji annotation, 3 Roadmap and 5 ChromHMM annotations and 5 other annotations (100 annotations total) (Table **??** and Table **??**).

We used two metrics to evaluate informativeness for disease heritability: enrichment and standardized effect size ($\tau^\star$). Enrichment is defined as the proportion of heritability explained by SNPs in an annotation divided by the proportion of SNPs in the annotation[33], and generalizes to annotations with values between 0 and 1[41]. Standardized effect size ($\tau^\star$) is defined as the proportionate change in per-SNP heritability associated with a 1 standard deviation increase in the value of the annotation, conditional on other annotations included in the model[34]; unlike enrichment, $\tau^\star$ quantifies effects that are unique to the focal annotation. In our "marginal" analyses, we estimated $\tau^\star$ for each focal annotation conditional on the baseline-LD-deep annotations. In our "joint" analyses, we merged baseline-LD-deep annotations with focal annotations that were marginally significant after Bonferroni correction and performed forward stepwise elimination to iteratively remove focal annotations that had conditionally non-significant $\tau^\star$ values after Bonferroni correction, as in ref.[34].

Enhancer-driven genes are uniquely informative for autoimmune disease heritability

We assessed the disease informativeness of 7 gene scores prioritizing Enhancer-driven genes in blood. We defined these gene scores based on distal connections, tissue-specific expression, or tissue-specific eQTL, all of which can characterize enhancer-driven regulation (Figure 1B, Table 1 and Methods). Some of these gene scores were derived from the same functional data that we used to define S2G strategies (e.g. ABC[42,43] and ATAC-seq[44]; see URLs). We included two published gene scores, (binarized) blood-specific enhancer domain score (EDS)[25] and specifically expressed genes in GTEx whole blood[9] (SEG-GTEx). The 7 Enhancer-driven gene scores were only weakly correlated (average $r = 0.04$) (Figure S3), implying that each score contains unique information about Enhancer-driven genes.

We combined the 7 Enhancer-driven gene scores with the 10 S2G strategies (Table 2) to define 70 annotations. In our marginal analysis using S-LDSC conditional on the baseline-LD+ model, all 70 enhancer-driven annotations were significantly enriched for

disease heritability, with larger enrichments for smaller annotations (Figure 3A and Table S5); values of standardized enrichment were more similar across annotations (Figure S4 and Table S6). 37 of the 70 enhancer-driven annotations attained conditionally significant $\tau^\star$ values after Bonferroni correction (Figure 3B and Table S5). We observed the strongest conditional signal for ATAC-distal × ABC ($\tau^* = 1.0 \pm 0.2$). ATAC-distal is defined by the proportion of mouse gene expression variability across blood cell types that is explained by distal ATAC-seq peaks in mouse[44]; the mouse genes are mapped to orthologous human genes. 4 of the 7 gene scores (ABC-G, ATAC-distal, EDS-binary and SEG-GTEx) produced strong conditional signals across many S2G strategies; however none of them attained Bonferonni-significant $\tau^\star$ for all 10 S2G strategies (Figure 3B). Among the S2G strategies, average conditional signals were strongest for the ABC strategy (average $\tau^* = 0.59$) and TSS strategy (average $\tau^* = 0.52$), which greatly outperformed the window-based S2G strategies (average $\tau^* = 0.04$-0.07), emphasizing the high added value of S2G strategies incorporating functional data (especially the ABC and TSS strategies).

We assessed the enrichment of the 7 Enhancer-driven gene scores (Table 1) in three disease-related gene sets: approved drug target genes for autoimmune diseases[10,45], "Bone Marrow/Immune" genes defined by the Developmental Disorders Database/Genotype-Phenotype Database (DDD/G2P)[46], and (top 10%) high-pLI genes[47] (Figure 3C and Table S7). 6 of the 7 gene scores were significantly enriched (after Bonferroni correction) in the drug target genes, 3 of 7 were significantly enriched in the immune genes, and 5 of 7 were significantly enriched in the high-pLI genes. The largest enrichment was observed for SEG-GTEx genes in the drug target genes (2.4x, s.e. 0.1).

We jointly analyzed the 37 enhancer-driven annotations that were Bonferonni-significant in our marginal analysis (Figure 3B and Table S5) by performing forward stepwise elimination to iteratively remove annotations that had conditionally non-significant τ^* values after Bonferroni correction. Of these, 6 annotations were jointly significant in the resulting Enhancer-driven joint model (Figure S5 and Table S8), corresponding to 4 Enhancer-driven gene scores: ABC-G, ATAC-distal, EDS-binary and SEG-GTEx.

We performed 2 secondary analyses. First, for each of the 6 annotations from the Enhancer-driven joint model (Figure S5), we assessed their functional enrichment for fine-mapped SNPs for blood-related traits from two previous studies[38,48]. We observed large and significant enrichments for all 6 annotations (Table S9), consistent with the S-LDSC results. Second, for each of the 7 Enhancer-driven gene scores, we performed pathway enrichment analyses to assess their enrichment in pathways from the ConsensusPathDB database[49]; all 7 gene scores were significantly enriched in immune-related and signaling pathways (Table S10).

We conclude that 4 of the 7 characterizations of Enhancer-driven genes are uniquely informative for autoimmune diseases and blood-related traits.

Genes with high network connectivity to Enhancer-driven genes are even more informative

We assessed the disease informativeness of a gene score prioritizing genes with high connectivity to Enhancer-driven genes in a protein-protein interaction (PPI) network (PPI-enhancer).We hypothesized that (i) genes that are connected to Enhancer-driven genes in biological networks are likely to be important, and that (ii) combining potentially

noisy metrics defining enhancer-driven genes would increase statistical signal. We used the STRING PPI network[26] to quantify the network connectivity of each gene with respect to each of the 4 uniquely informative Enhancer-driven gene scores from Figure S5 (ABC-G, ATAC-distal, EDS-binary and SEG-GTEx) (Figure 1D). Network connectivity scores were computed using a random walk with restart algorithm[10,50] (see Methods). We defined the PPI-enhancer gene score based on genes in the top 10% of average network connectivity across the 4 Enhancer-driven gene scores (Table 1). The PPI-enhancer gene score was only moderately positively correlated with the 4 underlying Enhancer-driven gene scores (average r=0.28; Figure S3).

We combined the PPI-enhancer gene score with the 10 S2G strategies (Table 2) to define 10 annotations. In our marginal analysis using S-LDSC conditional on the baseline-LD+ model, all 10 PPI-enhancer annotations were significantly enriched for disease heritability, with larger enrichments for smaller annotations (Figure 3A and Table S11); values of standardized enrichment were more similar across annotations (Figure S4 and Table S12). All 10 PPI-enhancer annotations attained conditionally significant τ^* values after Bonferroni correction (Figure 3B and Table S11). Notably, the maximum τ^* (2.0 (s.e. 0.3) for PPI-enhancer x ABC) was >2x larger than the maximum τ^* for the recently proposed Enhancer Domain Score[25] (EDS) (0.91 (s.e. 0.21) for EDS-binary x ABC). All 10 PPI-enhancer annotations remained significant when conditioned on the Enhancer-driven joint model from Figure S5 (Table S13).

We assessed the enrichment of the PPI-enhancer gene score in the three disease-related gene sets defined above (drug target genes[10,45], immune genes[46] and high-pLI genes[47]) (Figure 3C and Table S7). The PPI-enhancer gene score showed higher enrichment in all 3 gene sets compared to any of the 7 Enhancer-driven gene scores. In particular, the PPI-enhancer gene score was 5.3x (s.e. 0.1) enriched in drug target genes, a >2x stronger enrichment than the recently proposed Enhancer Domain Score[25] (EDS) (2.1x (s.e. 0.1)).

We jointly analyzed the 6 Enhancer-driven annotations from the Enhancer-driven joint model (Figure S5) and the 10 PPI-enhancer annotations from Table S13. Of these, 3 Enhancer-driven and 4 PPI-enhancer annotations were jointly significant in the resulting PPI-enhancer-driven joint model (Figure 3D and Table S14). The joint signal was strongest for PPI-enhancer $\times$ ABC ($\tau^\star = 1.2 \pm 0.21$), highlighting the informativeness of the ABC S2G strategy. 3 of the 7 annotations attained $\tau^\star > 0.5$; annotations with $\tau^* > 0.5$ are unusual, and considered to be important[51].

We sought to assess whether the PPI-enhancer disease signal derives from (i) the information in the PPI network or (ii) the improved signal-to-noise of combining different Enhancer-driven gene scores (see above). To assess this, we constructed an optimally weighted linear combination of the 4 enhancer-driven scores from Figure 3D, without using PPI network information (Weighted-enhancer; see Methods). We repeated the above analyses using Weighted-enhancer instead of PPI-enhancer. We determined that marginal $\tau^\star$ values were considerably lower for Weighted-enhancer vs. PPI-enhancer annotations (Table S15 vs. Table S11). (In addition, none of the Weighted-enhancer annotations were significant conditional on the PPI-enhancer-driven joint model from Figure 3D; see Table S16). This confirms that the additional PPI-enhancer signal derives from the information in the PPI network. To verify that the PPI-enhancer disease signal is driven not just by the PPI network but also by the input gene scores, we defined a new gene score analogous to PPI-enhancer but using 4 randomly generated binary gene sets of size 10% as input (PPI-control). We determined that marginal $\tau^\star$ values were overwhelmingly lower for PPI-control vs. PPI-enhancer annotations (Table S17 vs. Table

S11). (In addition, none of the PPI-control annotations were significant conditional on the PPI-enhancer-driven joint model from Figure 3D; see Table S18). This confirms that the PPI-enhancer disease signal is driven not just by the PPI network but also by the input gene scores.

We performed 3 secondary analyses. First, we defined a new gene score (RegNet-Enhancer) using the regulatory network from ref.[52] instead of the STRING PPI network, and repeated the above analyses. We determined that the STRING PPI network and the RegNet regulatory network are similarly informative (Table S19 and Table S20); we elected to use the STRING PPI network in our main analyses because the RegNet regulatory network uses GTEx expression data, which is also used by the SEG-GTEx gene score, complicating interpretation of the results. Second, for each of the 4 jointly significant PPI-enhancer annotations from Figure 3D, we assessed their functional enrichment for fine-mapped SNPs for blood-related traits from two previous studies[38,48]. We observed large and significant enrichments for all 4 annotations (Table S9), consistent with the S-LDSC results (and with the similar analysis of Enhancer-driven annotations described above). Third, we performed a pathway enrichment analysis to assess the enrichment of the PPI-enhancer gene score in pathways from the ConsensusPathDB database[49]; this gene score was enriched in immune-related pathways (Table S10).

We conclude that genes with high network connectivity to Enhancer-driven genes are uniquely informative for autoimmune diseases and blood-related traits, and strongly enriched for approved autoimmune disease drug target genes.

Master-regulator genes are uniquely informative for autoimmune disease heritability

We assessed the disease informativeness of two gene scores prioritizing Master-regulator genes in blood. We defined these gene scores using whole blood eQTL data from the eQTLGen consortium[53] (Trans-master-regulator) and a published list of known transcription factors in humans[54] (TF) (Figure 1C, Table 1 and Methods). We note that TF genes do not necessarily act as master regulators, but can be viewed as candidate master regulators. The two gene scores were only weakly correlated (r = 0.03) (Figure S3).

In detail, Trans-master-regulator is a binary gene score defined by genes that significantly regulate 3 or more other genes in trans via SNPs that are significant cis-eQTLs of the focal gene (10% of genes); the median value of the number of genes trans-regulated by a Trans-master-regulator gene is 14. Notably, trans-eQTL data from the eQTLGen consortium[53] was only available for 10,317 previously disease-associated SNPs. It is possible that genes with significant cis-eQTL that are disease-associated SNPs may be enriched for disease heritability irrespective of trans signals. To account for this gene-level bias, we conditioned all analyses of Trans-master-regulator annotations on both (i) 10 annotations based on a gene score defined by genes with at least 1 disease-associated cis-eQTL, combined with each of the 10 S2G strategies, and (ii) 10 annotations based on a gene score defined by genes with at least 3 unlinked disease-associated cis-eQTL, combined with each of the 10 S2G strategies; we chose the number 3 to maximize the correlation between this gene score and the Trans-master-regulator gene score ($r = 0.32$). Thus, our primary analyses were conditioned on 93 baseline-LD+ and 20 additional annotations (113 baseline-LD+cis model annotations); additional secondary analyses are described below. We did not consider a SNP annotation defined by trans-eQTLs,

because the trans-eQTLs in eQTLGen data were restricted to disease-associated SNPs, which would bias our results.

We combined the Trans-master-regulator gene score with the 10 S2G strategies (Table 2) to define 10 annotations. In our marginal analysis using S-LDSC conditional on the baseline-LD+cis model, all 10 Trans-master-regulator annotations were strongly and significantly enriched for disease heritability, with larger enrichments for smaller annotations (Figure 4A and Table S21); values of standardized enrichment were more similar across annotations (Figure S4 and Table S22). All 10 Trans-master-regulator annotations attained conditionally significant $\tau^\star$ values after Bonferroni correction (Figure 4B and Table S21). We observed the strongest conditional signals for Trans-master $\times$ TSS ($\tau^* = 1.6$, vs. $\tau^* = 0.37$-0.39 for Master-regulator $\times$ window-based S2G strategies). We observed similar (slightly more significant) results when conditioning on baseline-LD+ annotations only (Table S23).

As noted above, trans-eQTL data from the eQTLGen consortium[53] was only available for 10,317 previously disease-associated SNPs, and we thus defined and conditioned on baseline-LD+cis model annotations to account for gene-level bias. We verified that conditioning on annotations derived from gene scores defined by other minimum numbers of cis-eQTL and/or unlinked cis-eQTL produced similar results (Table S24, Table S25, Table S26, Table S27, Table S28). To verify that our results were not impacted by SNP-level bias, we adjusted each of the 10 Trans-master-regulator annotations by removing all disease-associated trans-eQTL SNPs in the eQTLGen data from the annotation, as well as any linked SNPs (Methods). We verified that these adjusted annotations produced similar results (Table S29).

TF is a binary gene score defined by a published list of 1,639 known transcription factors in humans[54]. We combined TF with the 10 S2G strategies (Table 2) to define 10 annotations. In our marginal analysis conditional on the baseline-LD+cis model, all 10 TF annotations were significantly enriched for heritability, but with smaller enrichments than the Trans-master-regulator annotations (Table S21); see Table S22 for standardized enrichments. 9 TF annotations attained significant $\tau^\star$ values after Bonferonni correction (Table S21) (the same 9 annotations were also significant conditional on the baseline-LD+ model; Table S23). Across all S2G strategies, $\tau^\star$ values of Trans-master-regulator annotations were larger than those of TF annotations (Table S21).

We assessed the enrichment of the Trans-master-regulator and TF gene scores in the three disease-related gene sets defined above (drug target genes[10,45], immune genes[46] and high-pLI genes[47] (Figure 4C and Table S7). The Trans-master-regulator gene score showed higher enrichment in all three gene sets compared to the TF gene score. The enrichments for master-regulator genes were lower in comparison to some Enhancer-driven genes and PPI-enhancer genes (Figure 3C); this can be attested to the fact that master-regulator genes may tend to disrupt genes across several pathways often rendering them unsuitable for drug targets.

We jointly analyzed the 10 Trans-master-regulator and 9 TF annotations that were Bonferroni-significant in our marginal analyses (Figure 4B and Table S21) by performing forward stepwise elimination to iteratively remove annotations that had conditionally non-significant τ^* values after Bonferroni correction. Of these, 3 Trans-master-regulator annotations and 2 TF annotations were jointly significant in the resulting Master-regulator joint model (Figure S6 and Table S30). The joint signal was strongest for Trans-master $\times$ Roadmap ($\tau^* = 0.81$, s.e. $= 0.13$), emphasizing the high added value of the Roadmap S2G strategy.

We performed 4 secondary analyses. First, for comparison purposes, we defined a binary gene score (Trans-regulated) based on genes with at least one significant trans-eQTL. We combined Trans-regulated genes with the 10 S2G strategies to define 10 annotations. In our marginal analysis using S-LDSC conditional on the baseline-LD+cis model, none of the Trans-regulated annotations attained conditionally significant $\tau^\star$ values after Bonferroni correction (Table S31). (In contrast, 3 of the annotations were significant when conditioning only on the baseline-LD+ model (Table S32).) This implies that genes that regulate other genes in *trans* are more disease-informative than genes that are regulated in *trans*. Second, a potential complexity is that trans-eQTL in whole blood may be inherently enriched for blood cell trait-associated SNPs (since SNPs that regulate the abundance of a specific blood cell type would result in trans-eQTL effects on genes that are specifically expressed in that cell type[53]), potentially limiting the generalizability of our results to non-blood cell traits. To ensure that our results were robust to this complexity, we verified that analyses restricted to the 5 autoimmune diseases (Table S1) produced similar results (Table S33). Third, for each of the 5 annotations from the Master-regulator joint model (Figure S6), we assessed their functional enrichment for fine-mapped SNPs for blood-related traits from two previous studies[38,48]. We observed large and significant enrichments for all 5 annotations (Table S9), consistent with the S-LDSC results (and with similar analyses described above). Fourth, we performed pathway enrichment analyses to assess the enrichment of the Trans-master-regulator and TF gene scores in pathways from the ConsensusPathDB database[49]. The Trans-master-regulator gene score was significantly enriched in immune-related pathways (Table S10).

We conclude that Master-regulator genes are uniquely informative for autoimmune diseases and blood-related traits.

Genes with high network connectivity to Master-regulator genes are even more informative

We assessed the disease informativeness of a gene score prioritizing genes with high connectivity to Master-regulator genes in the STRING PPI network[26] (PPI-master, analogous to PPI-enhancer; see Methods and Table 1). The PPI-master gene score was positively correlated with the 2 underlying master-regulator gene scores (average $r = 0.43$) and modestly correlated with PPI-enhancer (r=0.22) (Figure S3).

We combined the PPI-master gene score with the 10 S2G strategies (Table 2) to define 10 annotations. In our marginal analysis using S-LDSC conditional on the baseline-LD+cis model, all 10 PPI-master annotations were significantly enriched for disease heritability, with larger enrichments for smaller annotations (Figure 4A and Table S34); values of standardized enrichment were more similar across annotations (Figure S4 and Table S35). All 10 PPI-master annotations attained conditionally significant τ^* values after Bonferroni correction (Figure 4B and Table S34) (as expected, results were similar when conditioning only on the baseline-LD+ model; Table S36). We observed the strongest conditional signals for PPI-master combined with TSS ($\tau^\star$=1.7, s.e. 0.16), Coding ($\tau^\star$=1.7, s.e. 0.14) and ABC ($\tau^\star$=1.6, s.e. 0.17) S2G strategies, again emphasizing the high added value of S2G strategies incorporating functional data (Table S34). 9 of the 10 PPI-master annotations remained significant when conditioning on the Master-regulator joint model from Figure S6 (Table S37).

We assessed the enrichment of the PPI-master gene score (Table 1) in the three disease-related gene sets defined above (drug target genes[10,45], immune genes[46] and

high-pLI genes[47] (Figure 4C and Table S7). The PPI-master gene score showed higher enrichment in all 3 gene sets compared to either of the 2 Master-regulator gene scores. In particular, the PPI-master gene score was 2.7x (s.e. 0.1) enriched in drug target genes (vs. 5.3x (s.e. 0.1) for PPI-enhancer).

We jointly analyzed the 5 Master-regulator annotations from the Master-regulator joint model (Figure S6 and Table S30) and the 9 PPI-master annotations from Table S37. Of these, 2 Trans-master-regulator and 3 PPI-master annotations were jointly significant in the resulting PPI-master-regulator joint model (Figure 4D and Table S38). The joint signal was strongest for PPI-master × Roadmap ($\tau^\star = 0.94 \pm 0.14$),and 4 of the 5 annotations attained $\tau^\star > 0.5$.

We performed 2 secondary analyses. First, for each of the 3 jointly significant PPI-master annotations from Figure 4D, we assessed their functional enrichment for fine-mapped SNPs for blood-related traits from two previous studies[38,48]. We observed large and significant enrichments for all 3 annotations (Table S9), consistent with the S-LDSC results (and with similar analyses described above). Second, we performed a pathway enrichment analysis to assess the enrichment of the PPI-master gene score in pathways from the ConsensusPathDB database[49] and report the top enriched pathways (Table S10).

We conclude that genes with high network connectivity to Master-regulator genes are uniquely informative for autoimmune diseases and blood-related traits.

Combined joint model

We constructed a combined joint model containing annotations from the above analyses that were jointly significant, contributing unique information conditional on all other annotations. We merged the baseline-LD+cis model with annotations from the PPI-enhancer (Figure 3D) and PPI-master (Figure 4D) joint models, and performed forward stepwise elimination to iteratively remove annotations that had conditionally non-significant $\tau^\star$ values after Bonferroni correction. The combined joint model contained 8 new annotations, including 2 Enhancer-driven, 2 PPI-enhancer, 2 Trans-master and 2 PPI-master annotations (Figure 5 and Table S39). The joint signals were strongest for PPI-enhancer × ABC ($\tau^\star = 0.99$, s.e. 0.23) and PPI-master×Roadmap ($\tau^\star = 0.91$, s.e. 0.12) highlighting the importance of two distal S2G strategies, ABC and Roadmap; 5 of the 8 new annotations attained $\tau^\star > 0.5$. We defined a new metric quantifying the conditional informativeness of a heritability model (combined τ^*, generalizing the combined $\tau^\star$ metric of ref.[55] to more than two annotations; see Methods). As expected, the combined joint model attained a larger combined $\tau^\star$ (2.5, s.e. 0.24) than the PPI-enhancer (1.5, s.e. 0.15) or PPI-master (1.9, s.e. 0.14) joint models (Figure S7, Table S40, Table S41, Table S42).

We evaluated the combined joint model of Figure 5 (and other models) by computing $\log l_{\mathrm{SS}}$[56] (an approximate likelihood metric) relative to a model with no functional annotations ($\Delta \log l_{\mathrm{SS}}$), averaged across a subset of 6 blood-related traits (1 autoimmune trait and 5 blood cell traits) from the UK Biobank (Table S1). The combined joint model attained a +12.3% larger $\Delta \log l_{\mathrm{SS}}$ than the baseline-LD model (Table S43); most of the improvement derived from the 7 S2G annotations (Figure 2) and the 8 Enhancer-driven and Master-regulator annotations (Figure 5). The combined joint model also attained a 27.2% larger $\Delta \log l_{\mathrm{SS}}$ than the baseline-LD model in a separate analysis of 24 non-blood-related traits from the UK Biobank (Table S44) which had lower absolute

$\log l_{SS}$ values (Table S43), implying that value of the annotations introduced in this paper is not restricted to autoimmune diseases and blood-related traits.

We performed 4 secondary analyses. First, we investigated whether the 8 annotations of the combined joint model still contributed unique information after including the pLI gene score[47], which has previously been shown to be conditionally informative for disease heritability[40,41,57]. We confirmed that all 8 annotations from Figure 5 remained jointly significant (Figure S8 and Table S45). Second, we considered integrating PPI network information via a single gene score (PPI-all) instead of two separate gene scores (PPI-enhancer and PPI-master). We determined that the combined joint model derived from PPI-all attained a similar combined $\tau^\star$ (2.5, s.e. 0.22; Table S40; see Table S46 for individual $\tau^\star$ values) as the combined joint model derived from PPI-enhancer and PPI-master (2.5, s.e. 0.24; Table S40), and we believe it is less interpretable. Third, we constructed a less restrictive combined joint model by conditioning on the baseline-LD+ model instead of the baseline-LD+cis model. The less restrictive combined joint model included 1 additional annotation, SEG-GTEx $\times$ Coding (Table S47). This implies that the combined joint model is largely invariant to conditioning on the baseline-LD+ or baseline-LD+cis model. Fourth, we analyzed binarized versions of all 11 gene scores (Table 1) using MAGMA[58], an alternative gene set analysis method. 9 of the 11 gene scores produced significant signals (Table S48), 11 marginally significant gene scores (Figure 3 and Figure 4) and 5 gene scores included in the combined joint model of Figure 5 in the S-LDSC analysis. However, MAGMA does not allow for conditioning on the baseline-LD model, does not allow for joint analysis of multiple gene scores to assess joint significance, and does not allow for incorporation of S2G strategies.

We conclude that both Enhancer-driven genes and Master-regulator genes, as well as genes with high network connectivity to those genes, are jointly informative for autoimmune diseases and blood-related traits.

Discussion

We have assessed the contribution to autoimmune disease of Enhancer-driven genes and Master-regulator genes, incorporating PPI network information and 10 functionally informed S2G strategies. We determined that Enhancer-driven and Master-regulator genes are uniquely informative for human disease, and that PPI networks and S2G strategies magnify these signals. The resulting gene scores produced uniquely informative SNP annotations, improved heritability models, and strong enrichment for approved autoimmune disease drug targets. In particular, our PPI-enhancer gene score produced stronger signals than the recently proposed Enhancer Domain Score[25] (EDS).

Our work has several downstream implications. First, the PPI-enhancer gene score, which attained a particularly strong enrichment for approved autoimmune disease drug targets, will aid prioritization of drug targets, analogous to pLI[47] and LOEUF[59,60]. Second, our results implicate ABC and Roadmap strategies as highly informative distal S2G strategies and TSS as a highly informative proximal S2G strategy, motivating the use of these S2G strategies in other settings (e.g. CRISPR experiments). Third, our framework for gene set analysis incorporating S2G strategies (instead of conventional window-based approaches) will be broadly applicable to other gene sets and diseases. At the level of genes, our findings have immediate potential for improving probabilistic fine-mapping of transcriptome-wide association studies[61]. At the level of SNPs, our findings have immediate potential for improving functionally informed fine-mapping[48,62–64] (including

experimental follow-up[65]), polygenic localization[48], and polygenic risk prediction[66,67].

Our work has several limitations, representing important directions for future research. First, we restricted our analyses to Enhancer-driven and Master-regulator genes in blood, focusing on autoimmune diseases and blood-related traits; this choice was primarily motivated by the better representation of blood cell types in functional genomics assays and trans-eQTL studies. However, it will be valuable to extend our analyses to other tissues and traits as more functional data becomes available. Second, the trans-eQTL data from eQTLGen consortium[53] is restricted to 10,317 previously disease-associated SNPs; we modified our analyses to account for this bias. However, it would be valuable to extend our analyses to genome-wide trans-eQTL data at large sample sizes, if that data becomes available. Third, we investigated the 10 S2G strategies separately, instead of constructing a single optimal combined strategy. A comprehensive evaluation of S2G strategies, and a method to combine them, will be provided elsewhere (S. Gazal, unpublished data). Fourth, the forward stepwise elimination procedure that we use to identify jointly significant annotations[34] is a heuristic procedure whose choice of prioritized annotations may be close to arbitrary in the case of highly correlated annotations; however, the correlations between the gene scores, S2G strategies, and annotations that we analyzed were modest. Despite all these limitations, our findings expand and enhance our understanding of the regulatory processes impacting autoimmune disease.

Methods

Genomic annotations and the baseline-LD model

We define an annotation as an assignment of a numeric value to each SNP in a predefined reference panel (e.g., 1000 Genomes Project[36]; see URLs). Binary annotations can have value 0 or 1 only. Continuous-valued annotations can have any real value; our focus is on continuous-valued annotations with values between 0 and 1. Annotations that correspond to known or predicted function are referred to as functional annotations. The baseline-LD model (v.2.1) contains 86 functional annotations (see URLs). These annotations include binary coding, conserved, and regulatory annotations (e.g., promoter, enhancer, histone marks, TFBS) and continuous-valued linkage disequilibrium (LD)-related annotations.

Gene Scores

We define a gene score as an assignment of a numeric value between 0 and 1 to each gene; we primarily focus on binary gene sets defined by the top 10% of genes. We analyze a total of 11 gene scores (Table 1): 7 Enhancer-driven gene scores, 2 Master-regulator gene scores and 2 PPI-based gene scores (PPI-master, PPI-enhancer) that aggregate information across Enhancer-driven and Master-regulator gene scores. We scored 22,020 genes on chromosomes 1-22 from ref.[7] (see URLs). When selecting the top 10% of genes for a given score, we rounded the number of genes to 2,200.

The 7 Enhancer-driven gene scores are as follows:

- **ABC-G**: A binary gene score denoting genes that are in top 10% of the number of 'intergenic' and 'genic' Activity-by-Contact (ABC) enhancer to gene links in blood cell types, with average HiC score fraction > 0.015[42] (see URLs).
- **ATAC-distal**: A probabilistic gene score denoting the proportion of gene expression variance in 86 immune cell types in mouse, that is explained by the patterns of chromatin covariance of distal enhancer OCRs (open chromatin regions) to the gene, compared to chromatin covariance of OCRs that are near TSS of the gene and unexplained variances (see Figure 2 from[44]). The genes were mapped to their human orthologs using Ensembl biomaRt[68].
- **EDS-binary**: A binary gene score denoting genes that are in top 10% of the blood-specific Activity-based Enhancer Domain Score (EDS)[25] that reflects the number of conserved bases in enhancers that are linked to genes in blood related cell types as per the Roadmap Epigenomics Project[69,70] (see URLs).
- **eQTL-CTS**: A probabilistic gene score denoting the proportion of immune cell-type-specific eQTLs (with FDR adjusted p-value < 0.05 in one or two cell-types) across 15 different immune cell-types from the DICEdb project[71] (see URLs).
- **Expecto-MVP**: A binary gene score denoting genes that are in top 10% in terms of the magnitude of variation potential (MVP) in GTEx Whole Blood, which is the sum of the absolute values of all directional mutation effects within 1kb of the TSS, as evaluated by the Expecto method[7] (see URLs).

- **PC-HiC-distal**: A binary gene score denoting genes that are in top 10% in terms of the total number of Promoter-capture HiC connections across 17 primary blood cell-types.
- **SEG-GTEx**: A binary gene score denoting genes that are in top 10% in terms of the SEG t-statistic[9] score in GTEx Whole Blood.

The 2 Master-regulator gene scores are as follows:

- **Trans-master**: A binary gene score denoting genes with significant trait-associated cis-eQTLs in blood that also act as significant trans-eQTLs for at least 3 other genes based on data from eQTLGen Consortium[53]. The number of 3 was decided to make the size of the gene set close to 10%, which makes it easily comparable to some other gene sets.
- **TF**: A binary gene score denoting genes that act as human transcription factors[54].

The 2 PPI-based gene scores are as follows:

- **PPI-enhancer**: A binary gene score denoting genes in top 10% in terms of closeness centrality measure to the disease informative enhancer-regulated gene scores. To get the closeness centrality metric, we first perform a Random Walk with Restart (RWR) algorithm[50] on the STRING protein-protein interaction (PPI) network[26,72](see URLs) with seed nodes defined by genes in top 10% of the 4 enhancer-regulated gene scores with jointly significant disease informativeness (ABC-G, ATAC-distal, EDS-binary and SEG-GTEx). The closeness centrality score was defined as the average network connectivity of the protein products from each gene based on the RWR method.
- **PPI-master**: A binary gene score denoting genes in top 10% in terms of closeness centrality measure to the 2 disease informative master-regulator gene scores (Trans-master and TF). The algorithm was same as that of PPI-enhancer.

S2G strategies

We define a SNP-to-gene (S2G) linking strategy as an assignment of 0, 1 or more linked genes to each SNP with minor allele count ≥ 5 in a 1000 Genomes Project European reference panel[36]. We explored 10 SNP-to-gene linking strategies, including both distal and proximal strategies (Table 2). The proximal strategies included gene body $\pm$ 5kb; gene body $\pm$ 100kb; predicted TSS (by Segway[73,74]) ; coding SNPs; and promoter SNPs (as defined by UCSC[75,76]). The distal strategies included regions predicted to be distally linked to the gene by Activity-by-Contact (ABC) scores[42,43] (see below); regions predicted to be enhancer-gene links based on Roadmap Epigenomics data (Roadmap)[69,70,77]; regions in ATAC-seq peaks that are highly correlated to expression of a gene in mouse immune cell-types (ATAC)[44]; regions distally connected through promoter-capture Hi-C links (PC-HiC)[78]; and SNPs with fine-mapped causal posterior probability (CPP)[41] > 0.001 in GTEx whole blood (we use this thresholding on CPP to ensure adequate annotation size for annotations resulting from combining this S2G strategy with the gene scores studied in this paper).

Activity-by-Contact model predictions

We used the Activity-by-Contact (ABC) model (https://github.com/broadinstitute/ABC-Enhancer-Gene-Prediction) to predict enhancer-gene connections in each cell type, based on measurements of chromatin accessibility (ATAC-seq or DNase-seq) and histone modifications (H3K27ac ChIP-seq), as previously described[42,43]. In a given cell type, the ABC model reports an "ABC score" for each element-gene pair, where the element is within 5 Mb of the TSS of the gene.

For each cell type, we:

- Called peaks on the chromatin accessibility data using MACS2 with a lenient p-value cutoff of 0.1.
- Counted chromatin accessibility reads in each peak and retained the top 150,000 peaks with the most read counts. We then resized each of these peaks to be 500bp centered on the peak summit. To this list we added 500bp regions centered on all gene TSS's and removed any peaks overlapping blacklisted regions[79,80] (`https://sites.google.com/site/anshulkundaje/projects/blacklists`). Any resulting overlapping peaks were merged. We call the resulting peak set candidate elements.
- Calculated element Activity as the geometric mean of quantile normalized chromatin accessibility and H3K27ac ChIP-seq counts in each candidate element region.
- Calculated element-promoter Contact using the average Hi-C signal across 10 human Hi-C datasets as described below.
- Computed the ABC Score for each element-gene pair as the product of Activity and Contact, normalized by the product of Activity and Contact for all other elements within 5 Mb of that gene.

To generate a genome-wide averaged Hi-C dataset, we downloaded KR normalized Hi-C matrices for 10 human cell types (GM12878, NHEK, HMEC, RPE1, THP1, IMR90, HUVEC, HCT116, K562, KBM7). This Hi-C matrix (5 Kb) resolution is available here: `ftp://ftp.broadinstitute.org/outgoing/lincRNA/average_hic/average_hic.v2.191020.tar.gz`[42,81]. For each cell type we performed the following steps.

- Transformed the Hi-C matrix for each chromosome to be doubly stochastic.
- We then replaced the entries on the diagonal of the Hi-C matrix with the maximum of its four neighboring bins.
- We then replaced all entries of the Hi-C matrix with a value of NaN or corresponding to Knight–Ruiz matrix balancing (KR) normalization factors ¡ 0.25 with the expected contact under the power-law distribution in the cell type.
- We then scaled the Hi-C signal for each cell type using the power-law distribution in that cell type as previously described.
- We then computed the "average" Hi-C matrix as the arithmetic mean of the 10 cell-type specific Hi-C matrices.

In each cell type, we assign enhancers only to genes whose promoters are "active" (i.e., where the gene is expressed and that promoter drives its expression). We defined active promoters as those in the top 60% of Activity (geometric mean of chromatin accessibility and H3K27ac ChIP-seq counts). We used the following set of TSSs (one per gene symbol) for ABC predictions: `https://github.com/broadinstitute/ABC-Enhancer-Gene-Prediction/blob/v0.2.1/reference/RefSeqCurated.170308.bed.CollapsedGeneBounds.bed`. We note that this approach does not account for cases where genes have multiple TSSs either in the same cell type or in different cell types.

For intersecting ABC predictions with variants, we took the predictions from the ABC Model and applied the following additional processing steps: (i) We considered all distal element-gene connections with an ABC score ≥ 0.015, and all distal or proximal promoter-gene connections with an ABC score ≥ 0.1. (ii) We shrunk the ~500-bp regions by 150-bp on either side, resulting in a ~200-bp region centered on the summit of the accessibility peak. This is because, while the larger region is important for counting reads in H3K27ac ChIP-seq, which occur on flanking nucleosomes, most of the DNA sequences important for enhancer function are likely located in the central nucleosome-free region. (iii) We included enhancer-gene connections spanning up to 2 Mb.

Stratified LD score regression

Stratified LD score regression (S-LDSC) is a method that assesses the contribution of a genomic annotation to disease and complex trait heritability[33,34]. S-LDSC assumes that the per-SNP heritability or variance of effect size (of standardized genotype on trait) of each SNP is equal to the linear contribution of each annotation

$$var\left(\beta_j\right) := \sum_c a_{cj}\tau_c, \tag{1}$$

where a_{cj} is the value of annotation c for SNP j, where a_{cj} may be binary (0/1), continuous or probabilistic, and τ_c is the contribution of annotation c to per-SNP heritability conditioned on other annotations. S-LDSC estimates the τ_c for each annotation using the following equation

$$E\left[\chi_j^2\right] = N\sum_c l(j,c)\tau_c + 1, \tag{2}$$

where $l(j,c) = \sum_k a_{ck}r_{jk}^2$ is the *stratified LD score* of SNP j with respect to annotation c and r_{jk} is the genotypic correlation between SNPs j and k computed using data from 1000 Genomes Project[36] (see URLs); N is the GWAS sample size.

We assess the informativeness of an annotation c using two metrics. The first metric is enrichment (E), defined as follows (for binary and probabilistic annotations only):

$$E = \frac{\frac{h_g^2(c)}{h_g^2}}{\frac{\sum_j a_{cj}}{M}}, \tag{3}$$

where $h_g^2(c)$ is the heritability explained by the SNPs in annotation c, weighted by the annotation values.

The second metric is standardized effect size ($\tau^\star$) defined as follows (for binary, probabilistic, and continuous-valued annotations):

$$\tau_c^\star = \frac{\tau_c sd_c}{\frac{h_g^2}{M}}, \tag{4}$$

where sd_c is the standard error of annotation c, h_g^2 the total SNP heritability and M is the total number of SNPs on which this heritability is computed (equal to $5,961,159$ in our analyses). $\tau_c^\star$ represents the proportionate change in per-SNP heritability associated to a 1 standard deviation increase in the value of the annotation.

Combined $\tau^\star$

We defined a new metric quantifying the conditional informativeness of a heritability model (combined τ^*, generalizing the combined $\tau^\star$ metric of ref.[55] to more than two annotations. In detail, given a joint model defined by M annotations (conditional on a published set of annotations such as the baseline-LD model), we define

$$\tau_{comb}^\star = \sqrt{\sum_{m=1}^{M} \tau_m^{\star 2} + \sum_{m \neq l} r_{ml} \tau_m^\star \tau_l^\star} \tag{5}$$

Here r_{ml} is the pairwise correlation of the annotations m and l, and $r_{ml}\tau_m^\star\tau_l^\star$ is expected to be positive since two positively correlated annotations typically have the same direction of effect (resp. two negatively correlated annotations typically have opposite directions of effect). We calculate standard errors for $\tau_{comb}^\star$ using a genomic block-jackknife with 200 blocks.

Evaluating heritability model fit using SumHer logl_{SS}

Given a heritability model (e.g. the baseline-LD model or the combined joint model of Figure 5), we define the Δlog$l_{\rm SS}$ of that heritability model as the log$l_{\rm SS}$ of that heritability model minus the log$l_{\rm SS}$ of a model with no functional annotations (baseline-LD-nofunct; 17 LD and MAF annotations from the baseline-LD model[34]), where log$l_{\rm SS}$[56] is an approximate likelihood metric that has been shown to be consistent with the exact likelihood from restricted maximum likelihood (REML). We compute p-values for Δlog$l_{\rm SS}$ using the asymptotic distribution of the Likelihood Ratio Test (LRT) statistic: -2 log$l_{\rm SS}$ follows a χ^2 distribution with degrees of freedom equal to the number of annotations in the focal model, so that -2Δlog$l_{\rm SS}$ follows a χ^2 distribution with degrees of freedom equal to the difference in number of annotations between the focal model and the baseline-LD-nofunct model. We used UK10K as the LD reference panel and analyzed 4,631,901 HRC (haplotype reference panel[82]) well-imputed SNPs with MAF $\geq$ 0.01 and INFO $\geq$ 0.99 in the reference panel; We removed SNPs in the MHC region, SNPs explaining $>$ 1% of phenotypic variance and SNPs in LD with these SNPs.

We computed $\Delta \log l_{SS}$ for 8 heritability models:

- **baseline-LD model**: annotations from the baseline-LD model[34] (86 annotations).
- **baseline-LD+ model**: baseline-LD model plus 7 new S2G annotations not included in the baseline-LD model (93 annotations).
- **baseline-LD+Enhancer model**: baseline-LD model+ plus 6 jointly significant S2G annotations c corresponding to Enhancer-driven gene scores from Figure S5 (99 annotations).
- **baseline-LD+PPI-enhancer model**: baseline-LD model+ plus 7 jointly significant S2G annotations c corresponding to Enhancer-driven and PPI-enhancer gene scores from Figure 3D (100 annotations).
- **baseline-LD+cis model**: baseline-LD+ plus 20 S2G annotations used to correct for confounding in evaluation of Trans-master gene score (see Results) (113 annotations).
- **baseline-LD+Master model**: baseline-LD+cis plus 4 jointly significant Master-regulator S2G annotations from Figure S6 (117 annotations).
- **baseline-LD+PPI-master model**: baseline-LD+cis plus 4 jointly significant Master-regulator and PPI-master S2G annotations from Figure 4D (117 annotations).
- **baseline-LD+PPI-master model**: baseline-LD+cis plus 8 jointly significant Enhancer-driven, Master-regulator, PPI-enhancer and PPI-master S2G annotations from the final joint model in Figure 5 (121 annotations).

Data Availability

All summary statistics used in this paper are publicly available (see URLs). This work used summary statistics from the UK Biobank study (`http://www.ukbiobank.ac.uk/`). The summary statistics for UK Biobank is available online (see URLs). All gene sets, S2G annotations and SNP annotations resulting from combining gene sets with S2G annotations are publicly available here: `https://data.broadinstitute.org/alkesgroup/LDSCORE/Dey_Enhancer_MasterReg`

Code Availability

The codes used to generate SNP annotations from gene sets, and for performing PPI-informed integration of gene sets are available on Github: `https://github.com/kkdey/GSSG`.

URLs

- Gene scores, S2G links, annotations
  `https://data.broadinstitute.org/alkesgroup/LDSCORE/Dey_Enhancer_MasterReg`

- Github code repository and data
  `https://github.com/kkdey/GSSG`
- Activity-by-Contact (ABC) S2G links:
  `https://www.engreitzlab.org/resources`
- 1000 Genomes Project Phase 3 data:
  `ftp://ftp.1000genomes.ebi.ac.uk/vol1/ftp/release/20130502`
- UK Biobank summary statistics:
  `https://data.broadinstitute.org/alkesgroup/UKBB/`
- baseline-LD model annotations:
  `https://data.broadinstitute.org/alkesgroup/LDSCORE/`
- BOLT-LMM software:
  `https://data.broadinstitute.org/alkesgroup/BOLT-LMM`
- S-LDSC software:
  `https://github.com/bulik/ldsc`

Acknowledgments

We thank Sebastian Pott, John Platig, Xinchen Wang and Soumya Raychaudhuri for helpful discussions. This research was funded by NIH grants U01 HG009379, R01 MH101244, K99HG010160, R37 MH107649, R01 MH115676 and R01 MH109978. This research was conducted using the UK Biobank Resource under application 16549.

References

1. M.T. Maurano et al. Systematic localization of common disease-associated variation in regulatory DNA. *Science*, 337:1190–1195, 2012.
2. G. Trynka et al. Chromatin marks identify critical cell types for fine mapping complex trait variants. *Nature genetics*, 45(2):124–130, 2013.
3. J.K. Pickrell. Joint analysis of functional genomic data and genome-wide association studies of 18 human traits. *The American Journal of Human Genetics*, 94(4):559–573, 2014.
4. A.L. Price, C.C. Spencer, and P. Donnelly. Progress and promise in understanding the genetic basis of common diseases. *Proceedings of the Royal Society B: Biological Sciences*, 282(1821):20151684, 2015.
5. P.M. Visscher et al. 10 years of GWAS discovery: biology, function, and translation. *The American Journal of Human Genetics*, 101(1):5–22, 2017.
6. J. Shendure, G.M. Findlay, and M.W. Snyder. Genomic medicine–progress, pitfalls, and promise. *Cell*, 177:45–57, 2019.
7. J. Zhou, C.L. Theesfeld, K. Yao, K.M. Chen, A.K. Wong, and O.G. Troyanskaya. Deep learning sequence-based ab initio prediction of variant effects on expression and disease risk. *Nature genetics*, 50:1171–1179, 2018.

8. X. Zhu and M. Stephens. Large-scale genome-wide enrichment analyses identify new trait-associated genes and pathways across 31 human phenotypes. *Nature communications*, 9(1):4361, 2018.

9. H.K. Finucane, Y.A. Reshef, V. Anttila, K. Slowikowski, A. Gusev, A. Byrnes, et al. Heritability enrichment of specifically expressed genes identifies disease-relevant tissues and cell types. *Nature genetics*, 50:621–629, 2018.

10. H. Fang et al. A genetics-led approach defines the drug target landscape of 30 immune-related traits. *Nature genetics*, 51:1082–1091, 2019.

11. S.S. Kim et al. Genes with high network connectivity are enriched for disease heritability. *The American Journal of Human Genetics*, 104:896–913, 2019.

12. Q. Wang et al. A Bayesian framework that integrates multi-omics data and gene networks predicts risk genes from schizophrenia GWAS data. *Nature neuroscience*, 22:691–699, 2019.

13. C.S. Smillie et al. Intra-and inter-cellular rewiring of the human colon during ulcerative colitis. *Cell*, 178:714–730, 2019.

14. M. Wainberg et al. Opportunities and challenges for transcriptome-wide association studies. *Nature genetics*, 51:592–599, 2019.

15. A.D. Sawle et al. Identification of master regulator genes in human periodontitis. *Journal of dental research*, 95:1010–1017, 2016.

16. E.A. Boyle, Y.I. Li, and J.K. Pritchard. An expanded view of complex traits: from polygenic to omnigenic. *Cell*, 169:1177–1186, 2017.

17. B. Brynedal et al. Large-scale trans-eQTLs affect hundreds of transcripts and mediate patterns of transcriptional co-regulation. *The American Journal of Human Genetics*, 100(4):581–591, 2017.

18. C. Yao et al. Dynamic role of trans regulation of gene expression in relation to complex traits. *The American Journal of Human Genetics*, 100:571–580, 2017.

19. D.M.D. Vargas et al. Alzheimer's disease master regulators analysis: search for potential molecular targets and drug repositioning candidates. *Alzheimer's research & therapy*, 10:59, 2018.

20. L.E. Montefiori et al. A promoter interaction map for cardiovascular disease genetics. *Elife*, 7:e35788, 2018.

21. J.M. Karnuta and P.C. Scacheri. Enhancers: bridging the gap between gene control and human disease. *Human molecular genetics*, 27(R2):R219–R227, 2018.

22. X. Liu, Y.I. Li, and J.K. Pritchard. Trans effects on gene expression can drive omnigenic inheritance. *Cell*, 177:1022–1034, 2019.

23. A.D. Torshizi et al. Deconvolution of Transcriptional Networks Identifies TCF4 as a Master Regulator in Schizophrenia. *Science Advances*, 5:eaau4139, 2019.

24. R. Andersson and A. Sandelin. Determinants of enhancer and promoter activities of regulatory elements. *Nature Reviews Genetics*, pages 1–17, 2019.

25. X. Wang and D.B. Goldstein. Enhancer Domains Predict Gene Pathogenicity and Inform Gene Discovery in Complex Disease. *The American Journal of Human Genetics*, 106:215–233, 2020.

26. D. Szklarczyk et al. The STRING database in 2017: quality-controlled protein–protein association networks, made broadly accessible. *Nucleic acids research*, 45(Database issue):D362–D368, 2017.

27. T. Li and other. A scored human protein–protein interaction network to catalyze genomic interpretation. *Nature methods*, 14(1):61–64, 2017.

28. N.N. Parikshak, M.J. Gandal, and D.H. Geschwind. Systems biology and gene networks in neurodevelopmental and neurodegenerative disorders. *Nature Reviews Genetics*, 16(8):441–458, 2015.

29. M. Taşan and other. Selecting causal genes from genome-wide association studies via functionally coherent subnetworks. *Nature methods*, 12(2):154–159, 2015.

30. D. Marbach and other. Tissue-specific regulatory circuits reveal variable modular perturbations across complex diseases. *Nature methods*, 13(4):366–370, 2016.

31. L.A. Peters and other. A functional genomics predictive network model identifies regulators of inflammatory bowel disease. *Nature genetics*, 49(10):1437–1449, 2017.

32. X. Zhu, Z. Duren, and W.H. Wong. Modeling regulatory network topology improves genome-wide analyses of complex human traits. *bioRxiv*, 2020.

33. H.K. Finucane, B. Bulik-Sullivan, A. Gusev, G. Trynka, Y. Reshef, P.R. Loh, V. Anttila, H. Xu, C. Zang, K. Farh, and S. Ripke. Partitioning heritability by functional annotation using genome-wide association summary statistics. *Nature genetics*, 47:1228–1235, 2015.

34. S. Gazal et al. Linkage disequilibrium–dependent architecture of human complex traits shows action of negative selection. *Nature genetics*, 49(10):1421–1427, 2017.

35. S. Gazal, C. Marquez-Luna, H.K. Finucane, and A.L. Price. Reconciling s-ldsc and ldak models and functional enrichment estimates. *Nature genetics*, 51(8):1202–1204, 2019.

36. 1000 Genomes Project Consortium. A global reference for human genetic variation. *Molecular cell*, 526(7571):68–74, 2015.

37. T. Chen and C. Guestrin. Xgboost: A scalable tree boosting system. *In Proceedings of the 22nd acm sigkdd international conference on knowledge discovery and data mining*, ACM:785–794, 2016.

38. K.K.H. Farh et al. Genetic and epigenetic fine mapping of causal autoimmune disease variants. *Nature*, 518:337–343, 2015.

39. H. Huang et al. Fine-mapping inflammatory bowel disease loci to single-variant resolution. *Nature*, 547:173–178, 2017.

40. K.K. Dey et al. Evaluating the informativeness of deep learning annotations for human complex diseases. *bioRxiv (accepted in principle, Nat Commun)*, 2019.

41. F. Hormozdiari et al. Leveraging molecular quantitative trait loci to understand the genetic architecture of diseases and complex traits. *Nature genetics*, 50(7):1041–1047, 2018.

42. C.P. Fulco et al. Activity-by-contact model of enhancer–promoter regulation from thousands of CRISPR perturbations. *Nature Genetics*, 51:1664–1669, 2019.

43. J. Nasser et al. Genome-wide maps of enhancer regulation connect risk variants to disease genes. *bioRxiv*, 2020.

44. H. Yoshida et al. The cis-Regulatory Atlas of the Mouse Immune System. *Cell*, 176:897–912, 2019.

45. A. Gaulton et al. The ChEMBL database in 2017. *Nucleic acids research*, 45:D945–D954, 2016.

46. C.F. Wright et al. Genetic diagnosis of developmental disorders in the DDD study: a scalable analysis of genome-wide research data. *The Lancet*, 385(9975):1305–1314, 2015.

47. M. Lek, K.J. Karczewski, E.V. Minikel, K.E. Samocha, E. Banks, et al. Analysis of protein-coding genetic variation in 60,706 humans. *Nature*, 536:285–291, 2016.

48. O. Weissbrod et al. Functionally-informed fine-mapping and polygenic localization of complex trait heritability. *bioRxiv*, page p.807792, 2019.

49. A. Kamburov et al. The ConsensusPathDB interaction database: 2013 update. *Nucleic acids research*, 41(D1):D793–D800, 2012.

50. H. Tong, C. Faloutsos, and J.Y. Pan. Random walk with restart: fast solutions and applications. *Knowledge and Information Systems*, 14:327–346, 2008.

51. F.I. Hormozdiari et al. Functional disease architectures reveal unique biological role of transposable elements. *bioRxiv*, page p.482281, 2019.

52. A.R. Sonawane et al. Understanding tissue-specific gene regulation. *Cell reports*, 21:1077–1088, 2017.

53. U. Võsa et al. Unraveling the polygenic architecture of complex traits using blood eQTL meta-analysis. *bioRxiv*, page 447367, 2018.

54. S.A. Lambert et al. The human transcription factors. *Cell*, 172:650–665, 2018.

55. B. van de Geijn, H. Finucane, S. Gazal, F. Hormozdiari, T. Amariuta, and X Liu. Annotations capturing cell-type-specific TF binding explain a large fraction of disease heritability. *Human Molecular Genetics*, 29:1057–1067, 2020.

56. D. Speed, J. Holmes, and D.J Balding. Evaluating and improving heritability models using summary statistics. *Nature Genetics*, 52:458–462, 2020.

57. M.L. Hujoel et al. Disease heritability enrichment of regulatory elements is concentrated in elements with ancient sequence age and conserved function across species. *The American Journal of Human Genetics*, 104:611–624, 2019.

58. C.A. de Leeuw et al. MAGMA: generalized gene-set analysis of GWAS data. *PLoS computational biology*, 11(4):e1004219, 2015.

59. K.J. Karczewski et al. The mutational constraint spectrum quantified from variation in 141,456 humans. *Nature*, 581:434–443, 2020.

60. E.V. Minikel et al. Evaluating drug targets through human loss-of-function genetic variation. *Nature*, 581:459–464, 2020.

61. N. Mancuso et al. Probabilistic fine-mapping of transcriptome-wide association studies. *Nature genetics*, 51:675–682, 2019.

62. G. Kichaev et al. Integrating functional data to prioritize causal variants in statistical fine-mapping studies. *PLoS genetics*, 10(10):e1004722, 2014.

63. W. Chen et al. Incorporating functional annotations for fine-mapping causal variants in a Bayesian framework using summary statistics. *Genetics*, 204(3):933–958, 2016.

64. G. Kichaev et al. Improved methods for multi-trait fine mapping of pleiotropic risk loci. *Bioinformatics*, 33(2):248–255, 2017.

65. J.P. Ray et al. Prioritizing disease and trait causal variants at the TNFAIP3 locus using functional and genomic features. *Nature communications*, 11(1):1–13, 2020.

66. Y. Hu et al. Leveraging functional annotations in genetic risk prediction for human complex diseases. *PLoS computational biology*, 13(6):e1005589, 2017.

67. C. Márquez-Luna et al. Multiethnic polygenic risk scores improve risk prediction in diverse populations. *Genetic epidemiology*, 41(8):811–823, 2017.

68. R.J. Kinsella et al. Ensembl BioMarts: a hub for data retrieval across taxonomic space. *Database*, 2011.

69. A. Kundaje et al. Integrative analysis of 111 reference human epigenomes. *Nature*, 518:317–330, 2015.

70. Y. Liu, A. Sarkar, and M. Kellis. Evidence of a recombination rate valley in human regulatory domains. *Genome Biology*, page 193, 2017.

71. B.J. Schmiedel et al. Impact of genetic polymorphisms on human immune cell gene expression. *Cell*, 175:1701–1715, 2018.

72. D. Szklarczyk et al. STRING v10: protein–protein interaction networks, integrated over the tree of life. *Nucleic acids research*, 43:D447–D452, 2014.

73. M.M. Hoffman, J. Ernst, S.P. Wilder, A. Kundaje, R.S. Harris, and M. Libbrecht. A method to predict the impact of regulatory variants from DNA sequence. *Nucleic acids research*, 41:827–841, 2012.

74. M.M. Hoffman, O.J. Buske, J. Wang, Z. Weng, J.A. Bilmes, and W.S. Noble. Unsupervised pattern discovery in human chromatin structure through genomic segmentation. *Nature methods*, 9:473–476, 2012.

75. W.J. Kent et al. The human genome browser at ucsc. *Genome research*, 12(6):996–1006, 2002.

76. D. Karolchik et al. The ucsc table browser data retrieval tool. *Nucleic acids research*, 32 (Database Issue):D493–D496, 2004.

77. J. Ernst et al. Mapping and analysis of chromatin state dynamics in nine human cell types. *Nature*, 473:43–49, 2011.

78. B.M. Javierre et al. Lineage-specific genome architecture links enhancers and non-coding disease variants to target gene promoters. *Cell*, 167:1369–1384, 2016.

79. H.M. Amemiya, A. Kundaje, and A.P. Boyle. The ENCODE blacklist: identification of problematic regions of the genome. *Scientific reports*, 9(1):1–5, 2019.

80. ENCODE Project Consortium. An integrated encyclopedia of DNA elements in the human genome. *Nature*, 489:57–74, 2012.

81. Jan-Renier AJ Moonen et al. KLF4 Recruits SWI/SNF to Increase Chromatin Accessibility and Reprogram the Endothelial Enhancer Landscape under Laminar Shear Stress. *bioRxiv*, 2020.

82. S. McCarthy et al. A reference panel of 64,976 haplotypes for genotype imputation. *Nature genetics*, 48:1279–1283, 2016.

83. GTEx Consortium. Genetic effects on gene expression across human tissues. *Nature*, 550(7675):204–213, 2017.

84. C. Bycroft et al. The uk biobank resource with deep phenotyping and genomic data. *Nature*, 562(7726):203–209, 2018.

85. L. Jostins et al. Host-microbe interactions have shaped the genetic architecture of inflammatory bowel disease. *Nature*, 491:119–124, 2012.

86. Y. Okada et al. Genetics of rheumatoid arthritis contributes to biology and drug discovery. *Nature*, 506:376–381, 2014.

87. J. Bentham et al. Genetic association analyses implicate aberrant regulation of innate and adaptive immunity genes in the pathogenesis of systemic lupus erythematosus. *Nature genetics*, 47(12):1457–1464, 2015.

88. P.C. Dubois et al. Multiple common variants for celiac disease influencing immune gene expression. *Nature genetics*, 42(4):295–302, 2010.

89. A. Kamburov et al. ConsensusPathDB: toward a more complete picture of cell biology. *Nucleic acids research*, 39(suppl_1):D712–D717, 2010.

90. S.S. Kim et al. Improving the informativeness of Mendelian disease pathogenicity scores for common disease. *bioRxiv*, 2020.

Tables

Table 1. List of 11 gene scores: For each gene score, including (A) 7 Enhancer-driven genes scores (red font), (B) 2 Master-regulator gene scores (blue font) and (C) 2 PPI-network informed gene scores (corresponding to Enhancer-driven and Master-regulator gene scores), we provide a brief description and report its size (average gene score across 22,020 genes; equal to % of genes for binary gene scores). Gene scores are listed alphabetically within each category. All gene scores are binary except ATAC-distal and eQTL-CTS, which are probabilistic. Further details are provided in the Methods section.

Gene score	Description	Size (%)
(A) Enhancer-driven gene scores		
ABC-G	Genes in top 10% genes of number of genic and intergenic enhancer-gene connections in blood, assessed using Activity-By-Contact[42]	10%
ATAC-distal	Proportion of mouse gene expression variability across immune cell types explained by distal ATAC-seq peaks[44]	29%
EDS-binary*	Genes in top 10% of blood-specific Enhancer Domain Score (EDS), reflecting the number of bases in enhancers linked to a gene[25]	10%
eQTL-CTS	Proportion of eQTLs[71] (FDR < 0.05) that are specific to a single cell type (union across blood cell types).	32%
Expecto-MVP*	Genes in top 10% of magnitude of variation potential (MVP), based on Expecto Δ predictions of regions surrounding the TSS[7].	10%
PC-HiC-distal*	Genes in top 10% genes of number of distal Promoter Capture HiC (PC-HiC) connections in blood cell types[78].	10%
SEG-GTEx*	Specifically expressed genes[9](SEG) in GTEx whole blood[83]	10%
(B) Master-regulator gene scores		
Trans-master	Genes that significantly trans-regulate ≥ 3 genes by any significant cis-eQTL of the focal gene	10%
TF	Curated list of human Transcription Factor genes[54]	7.4%
(C) PPI network-based gene score		
PPI-enhancer	Genes with high network connectivity to Enhancer-driven genes in STRING[26] PPI network	10%
PPI-master	Genes with high network connectivity to Master-regulator genes in STRING[26] PPI network	10%

Table 2. List of 10 S2G strategies: For each S2G strategy, we provide a brief description, indicate whether the S2G strategy prioritizes distal or proximal SNPs relative to the gene, and report its size (% of SNPs linked to genes). S2G strategies are listed in order of increasing size. Further details are provided in the Methods section.

S2G strategy	Description	Distal/ Proximal	Size (%)
ABC	Inter-genic SNPs with distal enhancer-gene connections, assessed by Activity-By-Contact[42,43] across blood cell types.	Distal	1.4
TSS	SNPs in predicted Transcription start sites[73,74] overlapping Ensembl gene±5kb window.	Proximal	1.6
Coding	SNPs in coding regions	Proximal	1.6
ATAC	SNPs in ATAC-seq peaks >50% correlated to mouse expression across blood cell-types[44] (mapped to human).	Distal	1.6
eQTL	SNPs with fine-mapped causal posterior probability[41] (CPP) >0.001 in GTEx whole blood.	Distal +Proximal	2.4
Roadmap	SNPs in predicted enhancer-gene links, assessed using Roadmap Epigenomics data[70,77].	Distal	3.2
Promoter	SNPs in promoter regions.	Proximal	4.3
PC-HiC	Distal SNPs with Promoter Capture HiC (PC-HiC)[78] connections to promoter regions in blood cell-types.	Distal	27
5kb	SNPs in ±5kb window around gene body.	Proximal	53
100kb	SNPs in ±100kb window around gene body.	Distal	81

Figures

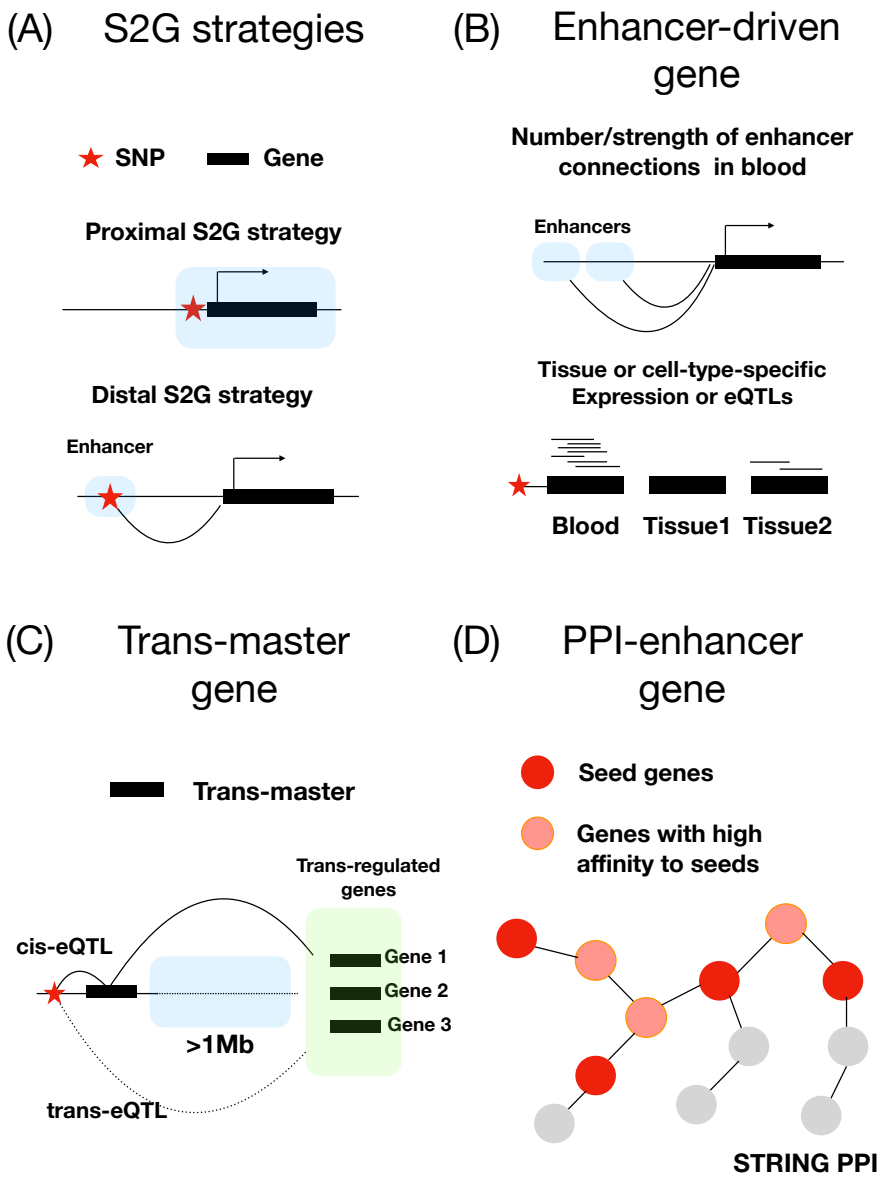

Figure 1. Illustration of S2G strategies and gene scores: (A) Proximal (close to gene body) and distal S2G strategies. (B) Examples of approaches used to define Enhancer-driven genes. (C) A Trans-master gene regulates multiple distal genes, via a cis-eQTL that is a trans-eQTL of the distal genes. (D) PPI-Enhancer genes have high connectivity to Enhancer-driven genes in a PPI network.

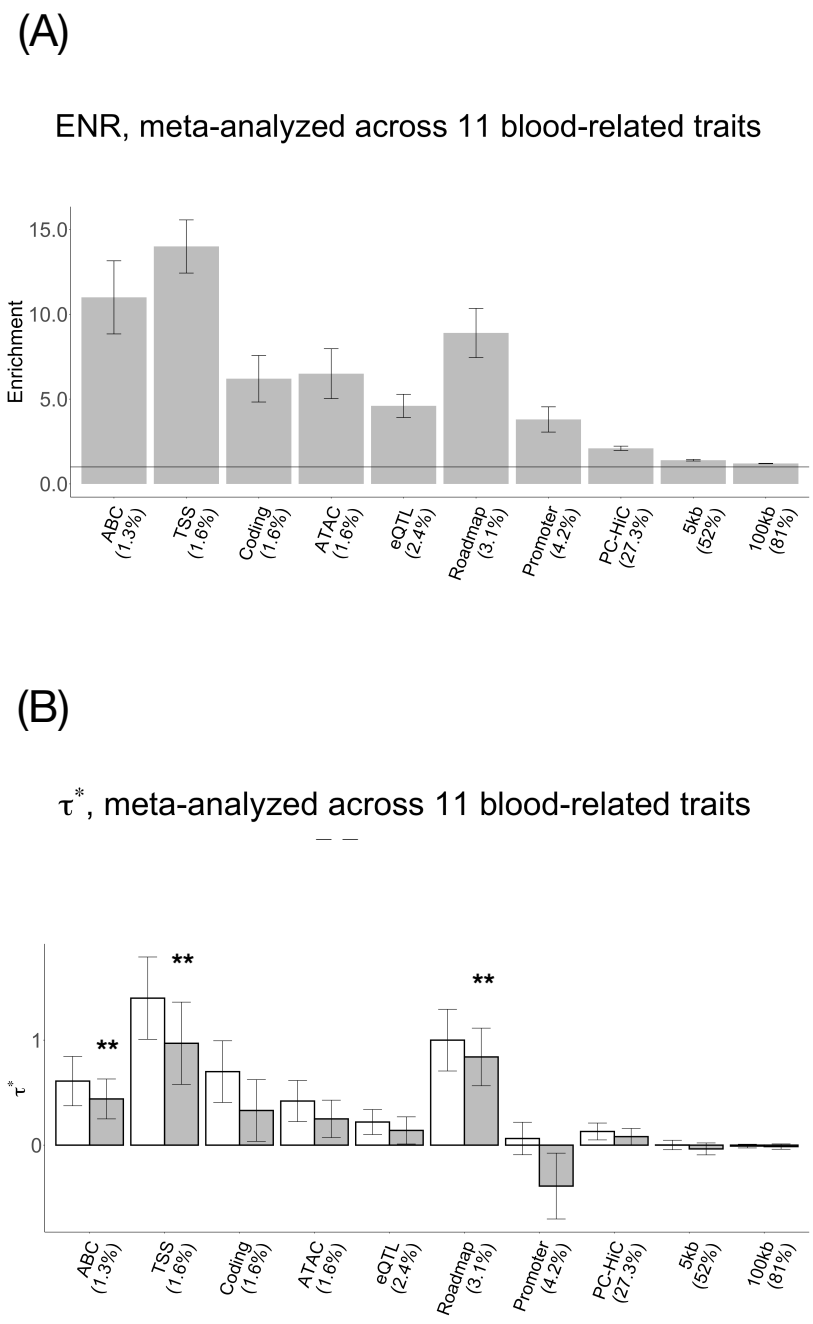

Figure 2. Disease informativeness of S2G annotations: We evaluated 10 S2G annotations, defined from the corresponding S2G strategies by SNPs linked to the set of all genes. (A) Heritabilty enrichment, conditional on the baseline-LD model. Horizontal line denotes no enrichment. (B) Standardized effect size ($\tau^\star$), conditional on either the baseline-LD model (marginal analyses: left column, white) or the baseline-LD+ model, which includes all 10 S2G annotations (right column, dark shading). Results are meta-analyzed across 11 blood-related traits. ** denotes $P < 0.05/10$. Error bars denote 95% confidence intervals. Numerical results are reported in Table S2 and Table S4.

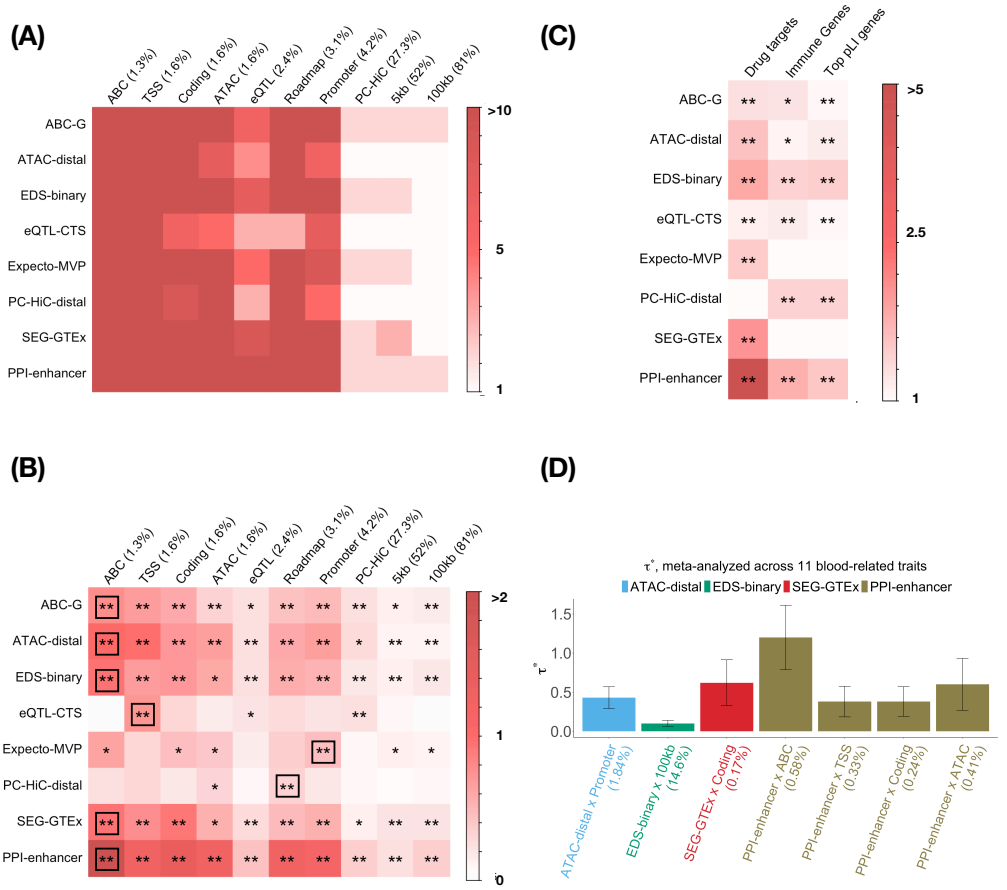

Figure 3. Disease informativeness of Enhancer-driven and PPI-enhancer annotations: We evaluated 80 annotations constructed by combining 7 Enhancer-driven + 1 PPI-enhancer gene sets with 10 S2G strategies.(A) Heritability enrichment, conditional on the baseline-LD+ model. (B) Standardized effect size ($\tau^\star$), conditional on the baselineLD+ model. (C) Enrichment of Enhancer-driven and PPI-enhancer genes in approved drug target genes[10,45], "Bone-marrow/Immune" genes in DDD/G2P database[46] and (top 10%) high-pLI genes[47]. (D) Standardized effect size ($\tau^\star$), conditional on the baseline-LD+ model plus 7 jointly significant Enhancer-driven + PPI-enhancer annotations. In panels A and B, results are meta-analyzed across 11 blood-related traits. In panels B and C, ** denotes Bonferroni-significant ($P < 0.05/110$) and * denotes FDR < 0.05. In panel B, the black box in each row denotes the S2G strategy with highest $\tau^\star$. Numerical results are reported in Table S5, Table S7, Table S11 and Table S14.

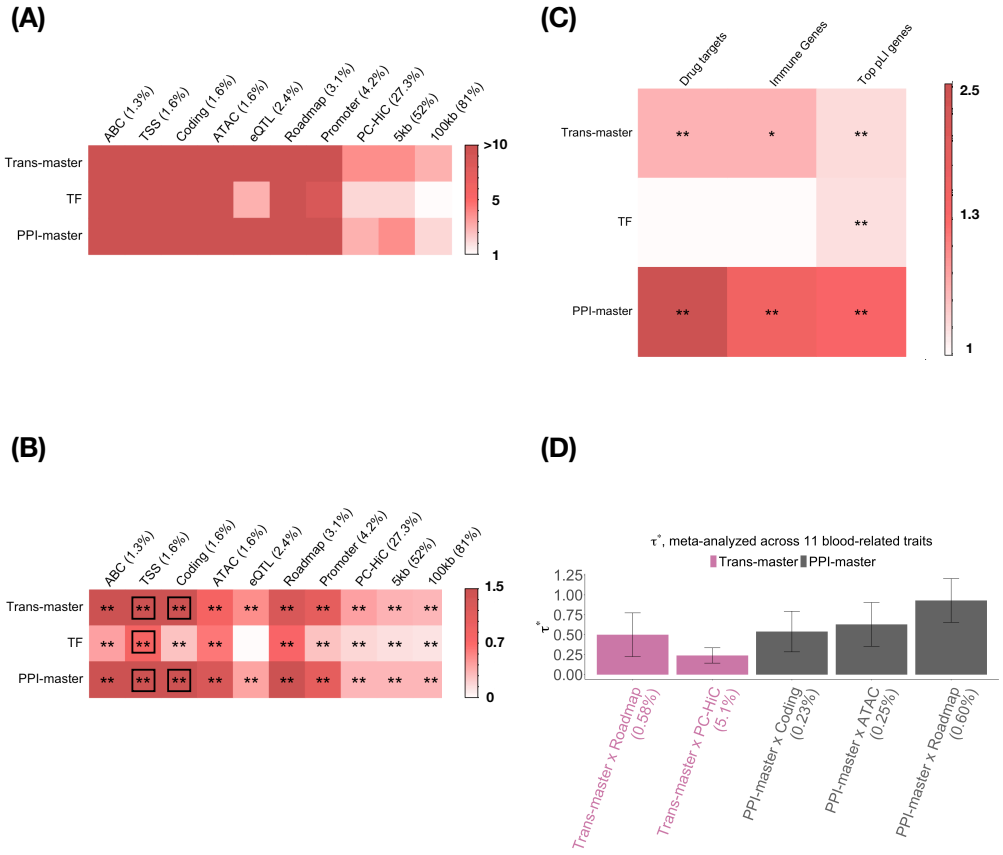

Figure 4. Disease informativeness of Master-regulator and PPI-master annotations: We evaluated 30 annotations constructed by combining 2 Master-regulator + 1 PPI-master gene sets with 10 S2G strategies. (A) Heritability enrichment, conditional on the baseline-LD+cis model. (B) Standardized effect size ($\tau^\star$), conditional on the baselineLD+cis model. (C) Enrichment of Master-regulator and PPI-master genes in approved drug target genes[10,45], "Bone-marrow/Immune" genes in DDD/G2P database[46] and (top 10%) high-pLI genes[47]. (D) Standardized effect size ($\tau^\star$), conditional on the baseline-LD+cis model plus 5 jointly significant Master-regulator + PPI-master annotations. In panels A and B, results are meta-analyzed across 11 blood-related traits. In panels B and C, ** denotes Bonferroni-significant ($P < 0.05/110$) and * denotes FDR < 0.05. In panel B, the black box in each row (or two black boxes in the case of a tie) denotes the S2G strategy with highest $\tau^\star$. Numerical results are reported in Table S21, Table S7, Table S34 and Table S38.

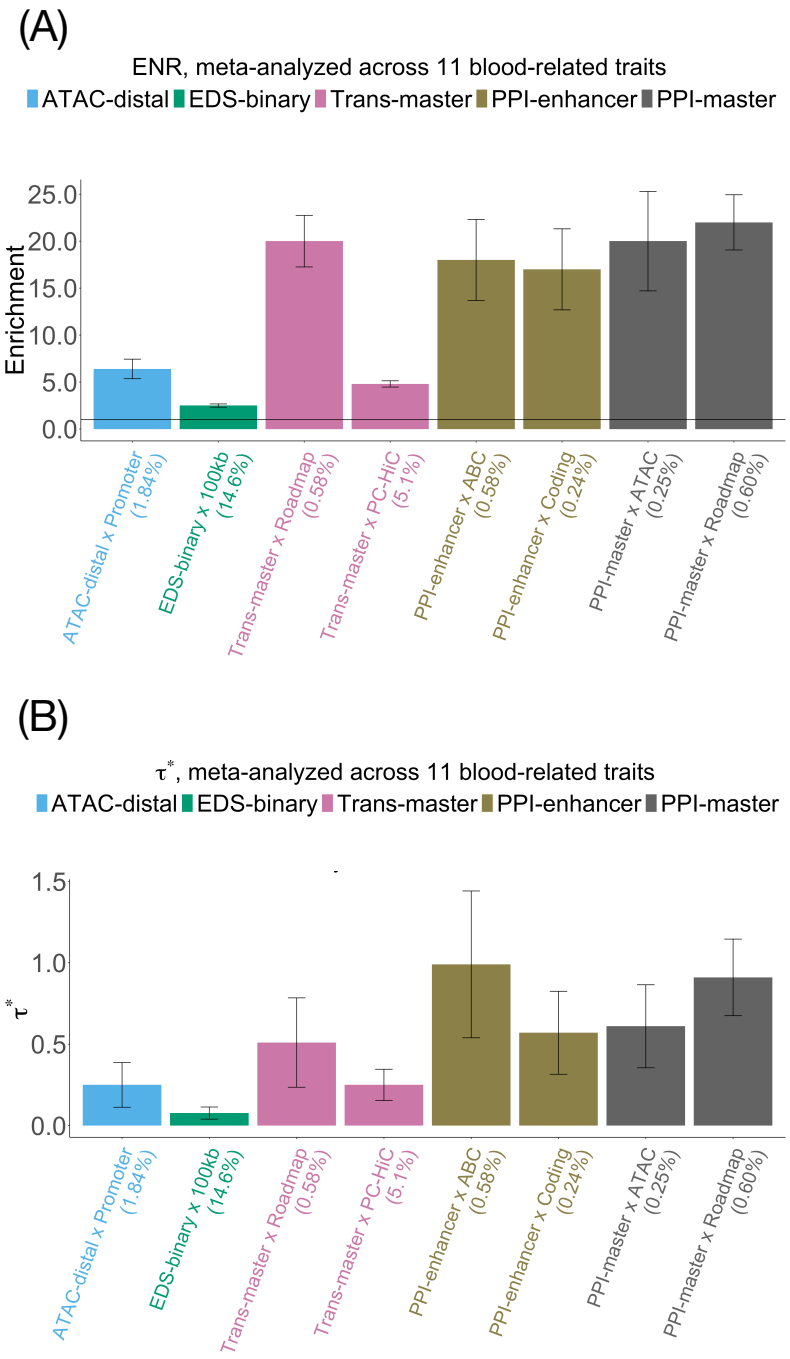

Figure 5. Combined joint model: (A) Heritability enrichment of the 8 jointly significant Enhancer-driven, Master-regulator, PPI-enhancer-driven and PPI-master-regulator annotations, conditional on the baseline-LD+cis model. Horizontal line denotes no enrichment. (B) Standardized effect size ($\tau^\star$) conditional on the baseline-LD+cis model plus the 8 jointly significant annotations. Errors bars denote 95% confidence intervals. Numerical results are reported in Table S39.

Supplementary Tables

Table S1. List of all blood-related traits: List of 11 blood-related traits (6 autoimmune diseases and 5 blood cell traits) analyzed in this paper.

Trait	Source	N
Auto Immune Traits (Sure)	UKBiobank[84]	459324
Crohn's Disease	Jostins et al., 2012 Nature[85]	20883
Rheumatoid Arthritis	Okada et al., 2014 Nature[86]	37681
Ulcerative Colitis	Jostins et al., 2012 Nature[85]	27432
Lupus	Bentham et al., 2015[87]	14267
Celiac	Dubois et al., 2010[88]	15283
Platelet Count	UKBiobank[84]	444382
Red Blood Cell Count	UKBiobank[84]	445174
Red Blood Cell Distribution Width	UKBiobank[84]	442700
Eosinophil Count	UKBiobank[84]	439938
White Blood Cell Count	UKBiobank[84]	444502

Table S2. S-LDSC results for SNPs linked to all genes conditional on baseline-LD model: Standardized Effect sizes ($\tau^\star$) and Enrichment (E) of 10 SNP annotations corresponding to all genes. The analysis is conditional on 86 baseline-LD (v2.1) annotations. Reports are meta-analyzed across 11 blood-related traits.

All genes						
Annotation	$\tau^\star$	se($\tau^\star$)	p($\tau^\star$)	E	se(E)	p(E)
ABC (1.3%)	0.61	0.12	1.4e-07	11	1.1	5.4e-08
TSS (1.6%)	1.4	0.2	2e-12	14	0.8	5.3e-08
Coding (1.6%)	0.70	0.15	4.5e-06	6.2	0.70	8e-05
ATAC (1.6%)	0.42	0.1	5.1e-05	6.5	0.75	1.3e-07
eQTL (2.4%)	0.22	0.061	0.00034	4.6	0.35	1.9e-06
Roadmap (3.1%)	1	0.15	3.6e-11	8.9	0.74	5e-11
Promoter (4.2%)	0.063	0.079	0.36	3.8	0.38	7.1e-05
PC-HiC (27.3%)	0.13	0.041	0.0018	2.1	0.065	1.4e-10
5kb (52%)	0.0013	0.023	0.95	1.4	0.025	6.9e-08
100kb (81%)	-0.009	0.0091	0.31	1.2	0.0067	8.9e-10

Table S3. Standardized enrichment of SNP annotations linked to all genes: Standardized enrichment of SNP annotations for SNPs linked to all genes, conditional on 86 baseline-LD annotations. Reports are meta-analyzed across 11 blood-related traits.

	All genes		
	$StdE$	se($StdE$)	p($StdE$)
ABC (1.3%)	1.3	0.12	7e-08
TSS (1.6%)	1.8	0.12	2.3e-07
Coding (1.6%)	0.87	0.092	4.7e-05
ATAC (1.6%)	0.81	0.093	1.2e-07
eQTL (2.4%)	0.69	0.055	2.9e-06
Roadmap (3.1%)	1.5	0.12	1e-10
Promoter (4.2%)	0.88	0.072	2.9e-05
PC-HiC (27.3%)	0.93	0.028	1.6e-10
5kb (52%)	0.69	0.013	5.3e-08
100kb (81%)	0.44	0.0026	8e-10

Table S4. S-LDSC results of a joint analysis of all S2G annotations for SNPs linked to all genes conditional on baseline-LD annotations: Standardized Effect sizes ($\tau^\star$) and Enrichment (E) of SNP annotations in a joint analysis comprising of 10 SNP annotations corresponding to all genes. The analysis is conditional on 86 baseline-LD annotations. Reports are meta-analyzed across 11 blood-related traits.

All genes						
Annotation	$\tau^\star$	se($\tau^\star$)	p($\tau^\star$)	E	se(E)	p(E)
ABC (1.3%)	0.44	0.097	4.8e-06	9.1	0.82	8.8e-07
TSS (1.6%)	0.97	0.2	1.6e-06	12	0.9	3e-06
Coding (1.6%)	0.33	0.15	0.022	5.1	0.69	0.00038
ATAC (1.6%)	0.25	0.091	0.0058	5.5	0.67	1.3e-06
eQTL (2.4%)	0.14	0.066	0.033	4.1	0.38	9.9e-06
Roadmap (3.1%)	0.84	0.14	6.1e-09	8	0.67	2.5e-10
Promoter (4.2%)	-0.39	0.16	0.01	3.2	0.47	0.00078
PC-HiC (27.3%)	0.081	0.04	0.043	2.1	0.06	2e-10
5kb (52%)	-0.036	0.029	0.21	1.4	0.028	8.4e-08
100kb (81%)	-0.014	0.013	0.27	1.2	0.0067	6.3e-10

Table S5. S-LDSC results for SNP annotations corresponding to Enhancer-driven gene scores: Standardized Effect sizes ($\tau^\star$) and Enrichment (E) of 70 SNP annotations corresponding to 7 Enhancer-driven gene scores and 10 S2G strategies, conditional on 93 baseline-LD+ annotations. Reports are meta-analyzed across 11 blood-related traits.

ABC-G

	$\tau^\star$	se($\tau^\star$)	p($\tau^\star$)	E	se(E)	p(E)
ABC (0.57%)	0.74	0.16	5.9e-06	15	1.5	2.4e-07
TSS (0.38%)	0.64	0.11	2.5e-08	19	1.8	2.7e-06
Coding (0.23%)	0.54	0.11	3.6e-07	16	2.1	6.7e-05
ATAC (0.30%)	0.28	0.073	0.00015	12	1.8	4.6e-06
eQTL (0.41%)	0.19	0.057	0.0012	7.4	0.98	2.7e-05
Roadmap (0.90%)	0.38	0.1	0.00017	12	1.3	1.4e-09
Promoter (0.60%)	0.44	0.082	8.3e-08	10	1.1	2.8e-05
PC-HiC (8.86%)	0.2	0.052	9.1e-05	3.1	0.17	8.2e-11
5kb (5.95%)	0.081	0.029	0.0057	3.1	0.13	1.1e-09
100kb (14.2%)	0.12	0.022	3.8e-08	2.6	0.095	1.2e-10

ATAC-distal

	$\tau^\star$	se($\tau^\star$)	p($\tau^\star$)	E	se(E)	p(E)
ABC (0.93%)	1.0	0.24	1.7e-05	12	1.1	1e-07
TSS (0.85%)	0.95	0.11	2.8e-17	16	1.1	2.4e-06
Coding (0.72%)	0.66	0.11	3.6e-09	11	1	2.5e-05
ATAC (1.02%)	0.63	0.15	1.9e-05	7.9	1	1.9e-07
eQTL (1.11%)	0.19	0.048	6.3e-05	5.4	0.44	4.6e-06
Roadmap (1.91%)	0.55	0.12	5.4e-06	9.6	0.86	1.6e-10
Promoter (1.84%)	0.63	0.073	3.3e-18	7.2	0.53	9.8e-06
PC-HiC (17.4%)	0.22	0.062	0.00027	2.5	0.089	1.3e-10
5kb (19.4%)	0.079	0.019	3.6e-05	2.1	0.037	1.2e-09
100kb (43.0%)	0.066	0.018	0.00021	1.8	0.036	1.4e-10

EDS-binary

	$\tau^\star$	se($\tau^\star$)	p($\tau^\star$)	E	se(E)	p(E)
ABC (0.44%)	0.91	0.21	1.4e-05	20	2.5	2.6e-07
TSS (0.26%)	0.64	0.12	1.6e-07	23	2.6	2.2e-06
Coding (0.22%)	0.66	0.1	1.6e-10	19	2.1	2.7e-05
ATAC (0.28%)	0.56	0.16	0.00042	15	2.8	2.9e-06
eQTL (0.32%)	0.18	0.042	2.6e-05	7.9	0.72	4.5e-06
Promoter (0.52%)	0.53	0.086	8.4e-10	12	1.2	2.3e-06
Roadmap (1.15%)	0.48	0.089	9.1e-08	11	0.98	2e-10
PC-HiC (7.63%)	0.15	0.041	0.00029	3	0.17	1.6e-10
5kb (5.66%)	0.096	0.02	1.6e-06	2.7	0.1	9e-10
100kb (14.6%)	0.15	0.02	6.4e-14	2.5	0.088	8.3e-11

eQTL-CTS

	$\tau^\star$	se($\tau^\star$)	p($\tau^\star$)	E	se(E)	p(E)
ABC (0.92%)	-0.047	0.22	0.83	9.8	0.9	2.6e-06
TSS (0.81%)	0.69	0.14	3.1e-07	14	1.2	9.9e-06
Coding (0.81%)	0.26	0.11	0.015	7.2	0.9	0.00025
ATAC (0.78%)	0.12	0.089	0.18	5.6	0.65	1.4e-05
eQTL (1.09%)	0.16	0.059	0.008	4.5	0.55	6.1e-05
Promoter (2.06%)	0.22	0.1	0.029	4.1	0.61	0.00072
Roadmap (1.56%)	0.16	0.11	0.15	8.3	0.68	5.3e-09

PC-HiC (17.0%)	0.18	0.046	0.00016	2.3	0.063	6.4e-10
5kb (22.2%)	0.053	0.02	0.0068	1.7	0.046	3.9e-08
100kb (50.2%)	-0.013	0.016	0.42	1.5	0.028	4.5e-10

Expecto-MVP

	$\tau^\star$	se($\tau^\star$)	p($\tau^\star$)	E	se(E)	p(E)
ABC (0.49%)	0.59	0.17	0.0004	16	2.1	3.2e-07
TSS (0.29%)	0.25	0.11	0.023	15	1.9	4.3e-05
Coding (0.21%)	0.41	0.15	0.0047	13	2.8	0.00044
ATAC (0.27%)	0.35	0.1	0.00069	13	2.3	3e-06
eQTL (0.38%)	0.11	0.047	0.018	6.3	0.71	1.8e-05
Roadmap (0.80%)	0.31	0.13	0.012	12	1.5	1.8e-09
Promoter (0.57%)	0.4	0.11	0.00015	9.1	1.1	1.6e-05
PC-HiC (7.08%)	0.03	0.05	0.55	2.8	0.18	7.9e-10
5kb (4.9%)	0.093	0.03	0.0021	2.9	0.16	3e-10
100kb (15.7%)	0.074	0.027	0.0064	2.3	0.086	3.8e-11

PC-HiC-distal

	$\tau^\star$	se($\tau^\star$)	p($\tau^\star$)	E	se(E)	p(E)
ABC (0.35%)	0.21	0.11	0.067	13	1.7	9.8e-06
TSS (0.24%)	0.26	0.099	0.0079	16	2	3.6e-05
Coding (0.20%)	0.14	0.1	0.18	9.3	2.2	0.002
ATAC (0.16%)	0.27	0.077	0.00052	13	1.8	2.1e-05
eQTL (0.34%)	0.04	0.049	0.41	4.5	0.65	8.4e-05
Roadmap (0.47%)	0.28	0.074	0.00017	11	1.1	3.4e-07
Promoter (0.49%)	0.14	0.079	0.083	5.9	0.96	0.00035
PC-HiC (12.0%)	0.029	0.042	0.49	2.4	0.098	3.4e-10
5kb (4.70%)	0.0091	0.018	0.61	2.2	0.083	1.5e-08
100kb (12.2%)	0.034	0.02	0.087	2	0.054	2.2e-09

SEG-GTEx

	$\tau^\star$	se($\tau^\star$)	p($\tau^\star$)	E	se(E)	p(E)
ABC (0.40%)	0.9	0.13	1.9e-11	20	1.8	1.7e-07
TSS (0.21%)	0.72	0.15	9.8e-07	26	3.1	1.6e-06
Coding (0.17%)	0.89	0.15	8.7e-09	24	3.2	1.8e-05
ATAC (0.26%)	0.51	0.15	0.00052	16	3	4.1e-06
eQTL (0.30%)	0.23	0.052	8.9e-06	8.9	1.1	4.8e-06
Roadmap (0.81%)	0.43	0.11	7.5e-05	12	1.3	1.7e-09
Promoter (0.50%)	0.51	0.073	4.1e-12	11	1	6e-06
PC-HiC (5.58%)	0.095	0.033	0.0044	3.2	0.2	9.9e-10
5kb (3.54%)	0.16	0.031	2.1e-07	3.7	0.26	9.1e-10
100kb (13.4%)	0.16	0.023	2.2e-11	2.4	0.096	2.5e-10

Table S6. Standardized enrichment of SNP annotations based on Enhancer-driven gene scores: Standardized enrichment of the enhancer-driven SNP annotations, conditional on 93 baseline-LD+ annotations. Reports are meta-analyzed across 11 blood-related traits.

ABC-G

	$StdE$	se($StdE$)	p($StdE$)
ABC (0.57%)	1.1	0.11	2.4e-07
TSS (0.38%)	1.2	0.11	2.7e-06
Coding (0.23%)	0.79	0.1	6.7e-05
ATAC (0.30%)	0.64	0.1	4.6e-06
eQTL (0.41%)	0.48	0.063	2.7e-05
Roadmap (0.90%)	1.1	0.12	1.4e-09
Promoter (0.60%)	0.77	0.082	2.8e-05
PC-HiC (8.86%)	0.88	0.049	8.2e-11
5kb (5.95%)	0.74	0.031	1.1e-09
100kb (14.2%)	0.92	0.033	1.2e-10

ATAC-distal

	$StdE$	se($StdE$)	p($StdE$)
ABC (0.93%)	1.2	0.11	1e-07
TSS (0.85%)	1.4	0.098	2.4e-06
Coding (0.72%)	0.89	0.085	2.5e-05
ATAC (1.02%)	0.79	0.1	1.9e-07
eQTL (1.11%)	0.55	0.045	4.6e-06
Roadmap (1.91%)	1.3	0.12	1.6e-10
Promoter (1.84%)	0.95	0.069	9.8e-06
PC-HiC (17.4%)	0.91	0.033	1.3e-10
5kb (19.4%)	0.82	0.014	1.2e-09
100kb (43.0%)	0.87	0.017	1.4e-10

EDS-binary

	$StdE$	se($StdE$)	p($StdE$)
ABC (0.44%)	1.3	0.16	2.6e-07
TSS (0.26%)	1.2	0.13	2.2e-06
Coding (0.22%)	0.89	0.098	2.7e-05
ATAC (0.28%)	0.83	0.16	3.1e-06
eQTL (0.32%)	0.44	0.04	4.5e-06
Promoter (0.52%)	0.83	0.09	2.3e-06
Roadmap (1.15%)	1.1	0.1	2e-10
PC-HiC (7.63%)	0.79	0.045	1.6e-10
5kb (5.66%)	0.63	0.024	9e-10
100kb (14.6%)	0.86	0.031	8.3e-11

eQTL-CTS

	$StdE$	se($StdE$)	p($StdE$)
ABC (0.92%)	0.9	0.082	2.6e-06
TSS (0.81%)	0.61	0.075	0.00025
Coding (0.81%)	0.61	0.075	0.00025
ATAC (0.78%)	0.45	0.052	1.4e-05
eQTL (1.09%)	0.41	0.05	6.1e-05
Promoter (2.06%)	0.54	0.081	0.00072
Roadmap (1.56%)	0.93	0.075	5.3e-09
PC-HiC (17.0%)	0.81	0.022	6.4e-10
5kb (22.2%)	0.62	0.017	3.9e-08

100kb (50.2%)	0.72	0.013	4.5e-10

Expecto-MVP

	StdE	se(*StdE*)	p(*StdE*)
ABC (0.49%)	1.1	0.15	3.2e-07
TSS (0.29%)	0.81	0.1	4.3e-05
Coding (0.21%)	0.62	0.13	0.00044
ATAC (0.27%)	0.67	0.12	3e-06
eQTL (0.38%)	0.39	0.044	1.8e-05
Roadmap (0.80%)	1	0.14	1.8e-09
Promoter (0.57%)	0.68	0.082	1.6e-05
PC-HiC (7.08%)	0.71	0.047	7.9e-10
5kb (4.9%)	0.62	0.034	3e-10
100kb (15.7%)	0.82	0.031	3.8e-11

PC-HiC-distal

	StdE	se(*StdE*)	p(*StdE*)
ABC (0.35%)	0.75	0.1	9.8e-06
TSS (0.24%)	0.77	0.096	3.6e-05
Coding (0.20%)	0.42	0.097	0.002
ATAC (0.16%)	0.51	0.073	2.1e-05
eQTL (0.34%)	0.26	0.038	8.4e-05
Roadmap (0.47%)	0.76	0.074	3.4e-07
Promoter (0.49%)	0.41	0.067	0.00035
PC-HiC (12.0%)	0.77	0.032	3.4e-10
5kb (4.70%)	0.47	0.018	1.5e-08
100kb (12.2%)	0.65	0.017	2.2e-09

SEG-GTEx

	StdE	se(*StdE*)	p(*StdE*)
ABC (0.40%)	1.3	0.11	1.7e-07
TSS (0.21%)	1.2	0.14	1.6e-06
Coding (0.17%)	0.98	0.13	1.8e-05
ATAC (0.26%)	0.8	0.15	4.1e-06
eQTL (0.30%)	0.49	0.058	4.8e-06
Roadmap (0.81%)	1.1	0.12	1.7e-09
Promoter (0.50%)	0.74	0.072	6e-06
PC-HiC (5.58%)	0.74	0.045	9.9e-10
5kb (3.54%)	0.68	0.048	9.1e-10
100kb (13.4%)	0.82	0.032	2.5e-10

Table S7. Enrichment of gene scores with disease associated genes, drug target genes and high pLI genes: Enrichment and bootstrap standard error of all probabilistic gene scores with respect to (a) genes that are Phase2+ drug targets for immune related diseases[10,45], (b) genes with "Bone Marrow/Immune" organ specific functionality as per the DDD/G2P scoring scheme[46] and (c) top 10 % pLI genes[47].

Gene Score	Immune drug targets	DDD/G2P (Bone Marrow, Immune)	Top 10% pLI
ABC-G	1.39 (0.07)	1.35 (0.19)	1.11 (0.04)
ATAC-distal	1.79 (0.04)	1.15 (0.08)	1.21 (0.02)
EDS-binary	2.14 (0.10)	1.57 (0.19)	1.61 (0.06)
eQTL-CTS	1.16 (0.03)	1.23 (0.06)	1.07 (0.01)
Expecto-MVP	1.67 (0.09)	0.97 (0.15)	0.60 (0.04)
PC-HiC-distal	0.91 (0.07)	1.57 (0.22)	1.57 (0.05)
SEG-GTEx	2.42 (0.11)	0.75 (0.16)	0.30 (0.03)
Trans-master	1.42 (0.07)	1.42 (0.18)	1.20 (0.05)
TF	0.53 (0.08)	1.01 (0.23)	1.16 (0.06)
PPI-enhancer	5.26 (0.12)	2.03 (0.22)	1.72 (0.05)
PPI-master	2.71 (0.11)	2.03 (0.22)	1.90 (0.06)

Table S8. S-LDSC results for joint analysis of all marginally significant SNP annotations for Enhancer-driven genes. Standardized Effect sizes ($\tau^\star$) and Enrichment (E) of the jointly significant Enhancer-driven SNP annotations from Table S5, conditional on the baseline-LD+ model and all SNP annotations in the Enhancer-driven joint model. Results are meta-analyzed across 11 blood-related traits.

Annotation	$\tau^\star$	se($\tau^\star$)	p($\tau^\star$)	E	se (E)	p(E)
ABC-G × TSS (0.38%)	0.56	0.11	6.1e-07	18	1.7	3.1e-06
ATAC-distal × Promoter (1.84%)	0.56	0.072	7.7e-15	6.9	0.51	1.2e-05
EDS-binary × Roadmap (1.15%)	0.31	0.088	0.00041	8.6	0.89	3.2e-09
EDS-binary × 100kb (14.6%)	0.096	0.02	2.4e-06	2.5	0.089	8.2e-11
SEG-GTEx × ABC (0.40%)	0.68	0.13	2.1e-07	17	1.8	9.1e-07
SEG-GTEx × Coding (0.17%)	0.68	0.15	8.3e-06	20	3.2	8.6e-05

Table S9. Enrichment of SNP annotations from different joint models with respect to fine-mapped SNPs for blood-related traits: We report the enrichment (E) and Jack-knife standard error with respect to 8,741 fine-mapped SNPs in autoimmune traits (Farh[38]) and 1,429 genome-wide functionally fine-mapped SNPs in blood-related traits[48].

Enhancer-driven joint model annotations: Figure S5

	Farh SNPs		Omer SNPs	
Annotation	E	se(E)	E	se(E)
ABC-G × TSS	5.67	0.26	12.5	0.41
ATAC-distal × Promoter	3.02	0.1	7.61	0.13
EDS-binary × Roadmap	5.67	0.17	5.60	0.13
EDS-binary × 100kb	2.22	0.04	2.00	0.02
SEG-GTEx × ABC	6.23	0.30	6.12	0.28
SEG-GTEx × Coding	7.60	0.41	14.0	1.16

Master regulator joint model annotations: Figure S6

	Farh SNPs		Omer SNPs	
Annotation	E	se(E)	E	se(E)
Trans-master × Roadmap	10.6	0.43	12.4	0.52
Trans-master × PC-HiC	5.1	0.22	3.5	0.08
Trans-master × 5kb	5.4	0.14	4.4	0.08
TF × ATAC	6.3	0.37	8.6	.0.40
TF × Roadmap	7.3	0.36	8.3	0.35

PPI-enhancer-driven joint model annotations: Figure 3D

	Farh SNPs		Omer SNPs	
Annotation	E	se(E)	E	se(E)
PPI-enhancer × ABC	9.0	0.50	8.7	0.32
PPI-enhancer × Coding	6.9	0.28	21.2	0.82
PPI-enhancer × ATAC	7.2	0.20	9.8	0.41
PPI-enhancer × TSS	6.5	0.28	16.1	0.51

PPI-master-regulator joint model annotations: Figure 4D

	Farh SNPs		Omer SNPs	
Annotation	E	se(E)	E	se(E)
PPI-master × Coding	7.1	0.37	22.9	0.95
PPI-master × ATAC	9.8	0.32	14.8	0.90
PPI-master × Roadmap	10.4	0.50	10.3	0.40

Table S10. Pathway enrichment analysis of the different gene scores: Pathway enrichment analysis of the top 10% genes for 7 Enhancer-driven gene scores (colored red), 2 Master-regulator gene scores (colored blue), PPI-enhancer and PPI-master gene scores (Methods). Pathway enrichment is performed using the ConsensusPathDB database[49,89]. Only the top 5 non-redundant and statistically significant (q-value < 0.05) pathways for a gene set are reported.

Gene Set	Top pathways
ABC-G	EGFR1 (7.1e-10), T cell receptor (8.5e-10), Neutrophil degranulation (9.8e-10), Interleukin signaling (2.2e-09), B cell receptor (4.2e-09)
ATAC-distal	Immune system (1.6e-11), Pathways in cancer(6.8e-10), White fat cell differentiation (5.5e-08),Cytokine signaling immune system (4.9e-07), EGFR1 (2.9e-06)
EDS-binary	T cell signaling (1.3e-12), T-cell receptor (1.3e-11), Th17 cell differentiation (8.8e-10), Hematopoeitic cell lineage (1.5e-09), Pathways in cancer (1.9e-09)
eQTL-CTS	Olfactory Receptor Activity (3e-03), GPCR signaling (0.01), RUNX1 HSC differentiation (0.01)
Expecto-MVP	Immune system (7.3e-38), cytokine signaling (3.8e-26), interferon signaling (1.8e-13), Innate immune system (2.0e-13), Neutrophil degranulation (8.4e-13)
PC-HiC-distal	HDACs deacetylate histones (1.0e-20), HATs acetylate histones (3.7e-20), ERCC6 and EHM2 rRNA regulation (5.8e-19), chromatin organization (1.9e-18), RNA Pol 1 transcription (1.1e-17)
SEG-GTEx	Immune system (5.9e-99), Neutrophil degranulation (6.8e-55), Cytokine signaling (1.5e-24), NK cell mediated toxicity (3.6e-18), Hematopoietic cell lineage (1.6e-17)
Trans-Master	Antigen processing and presentation (1.4e-17), Immune system (1.5e-13), Interferon gamma signaling (9.5e-11), Graft-versus-host disease (2.9e-10), Cytokine signaling (3.7e-10)
TF	Transcription pathway (2.4e-265), Neural receptor (1.9e-38), Transcription mis-regulation cancer (5.9e-25), Neural crest differentiation (4.3e-23), Adipogenesis (6.8e-22)
PPI-enhancer	Pathways in cancer (1.4e-119), Immune system (2.5e-116), Signal transduction (9.5e-112), Cytokine signaling immune system (7.7e-91), Innate immune system (5.5e-72)
PPI-master	Transcription pathway (8.1e-123), T-cell leukemia virus (7.0e-57), Viral carcinogenesis (5.7e-45), Hepatitis B (4.8e-43), JAK-STAT (6.3e-30)

Table S11. S-LDSC results for SNP annotations corresponding to the PPI-enhancer gene score conditional on the baseline-LD+ model: Standardized Effect sizes ($\tau^\star$) and Enrichment (E) of 10 SNP annotations corresponding to the PPI-enhancer gene score, conditional on 93 baseline-LD+ annotations. Reports are meta-analyzed across 11 blood-related traits.

	PPI-Enhancer					
	$\tau^\star$	se($\tau^\star$)	p($\tau^\star$)	E	se(E)	p(E)
ABC (0.58%)	2.0	0.29	8.2e-13	24	2.6	3.4e-09
TSS (0.33%)	1.2	0.17	2.6e-13	28	2.8	3.3e-08
Coding (0.24%)	1.4	0.18	4.8e-15	29	3	2.6e-08
ATAC (0.41%)	1.2	0.21	2.9e-08	20	2.9	2.9e-09
eQTL (0.38%)	0.39	0.085	4e-06	9.7	1.2	6.8e-08
Roadmap (1.05%)	1.2	0.18	3.4e-11	15	1.6	9e-12
Promoter (0.64%)	1.1	0.14	1e-14	15	1.3	2.1e-08
PC-HiC (8.66%)	0.32	0.056	1.1e-08	3.3	0.18	7.3e-11
5kb (6.45%)	0.21	0.022	4.3e-21	3.1	0.11	4.3e-10
100kb (17.3%)	0.31	0.026	5.1e-32	2.7	0.087	8.3e-11

Table S12. Standardized enrichment of SNP annotations corresponding to PPI-enhancer gene score conditional on the baseline-LD+ model: Standardized enrichment of the 10 SNP annotations corresponding to the PPI-enhancer gene score, conditional on 93 baseline-LD+ annotations respectively. Reports are meta-analyzed across 11 blood-related traits.

	PPI-enhancer		
	$StdE$	se($StdE$)	p($StdE$)
ABC (0.58%)	1.8	0.2	3.4e-09
TSS (0.33%)	1.6	0.16	3.3e-08
Coding (0.24%)	1.5	0.15	2.6e-08
ATAC (0.41%)	1.2	0.19	2.9e-09
eQTL (0.38%)	0.6	0.074	6.8e-08
Roadmap (1.05%)	1.5	0.16	9e-12
Promoter (0.64%)	1.2	0.1	2.1e-08
PC-HiC (8.66%)	0.92	0.05	7.3e-11
5kb (6.45%)	0.76	0.027	4.3e-10
100kb (17.3%)	1	0.033	8.3e-11

Table S13. S-LDSC results for SNP annotations corresponding to the PPI-enhancer gene score conditional on the Enhancer-driven joint model: Standardized Effect sizes ($\tau^\star$) and Enrichment (E) of 10 SNP annotations corresponding to the PPI-enhancer gene score, conditional on the Enhancer-driven joint model from Table S8. Reports are meta-analyzed across 11 blood-related traits.

	PPI-enhancer					
	$\tau^\star$	se($\tau^\star$)	p($\tau^\star$)	E	se(E)	p(E)
ABC (0.58%)	1.8	0.3	3.5e-09	21	2.5	8.4e-09
TSS (0.33%)	0.85	0.15	4.6e-08	24	2.6	9.9e-08
Coding (0.24%)	0.93	0.16	3.1e-09	25	2.9	1.2e-07
ATAC (0.41%)	0.96	0.2	1.8e-06	17	2.8	3.6e-08
eQTL (0.38%)	0.29	0.08	0.00024	8.7	1.2	2.9e-07
Roadmap (1.05%)	1	0.18	4.5e-08	13	1.5	4.9e-11
Promoter (0.64%)	0.73	0.14	2e-07	13	1.3	7.7e-08
PC-HiC (8.66%)	0.24	0.053	4.5e-06	3.1	0.17	8e-11
5kb (6.45%)	0.13	0.023	1.6e-08	3.2	0.11	4e-10
100kb (17.3%)	0.23	0.024	9.8e-23	2.7	0.087	8.6e-11

Table S14. S-LDSC results for the joint analalysis of SNP annotations corresponding to the Enhancer-driven and PPI-enhancer gene scores. Standardized Effect sizes ($\tau^\star$) and Enrichment (E) of the significant SNP annotations in a joint model comprising of marginally significant Enhancer-driven SNP annotations and PPI-enhancer SNP annotations and from Figure 3. We report results on the annotations that are significant in the joint model. Also marked in red are annotations that ere jointly Bonferroni significant in the Enhancer-driven joint model (Figure S5) but not Bonferroni significant in this PPI-enhancer-driven joint model. All analysis are conditional on 93 baseline-LD+ annotations. Results are meta-analyzed across 11 blood-related traits.

Annotation	$\tau^\star$	se($\tau^\star$)	p($\tau^\star$)	E	se (E)	p(E)
ATAC-distal × Promoter (1.8%)	0.43	0.071	1.1e-09	6.7	0.51	1.6e-05
EDS-binary × 100kb (14.6%)	0.10	0.02	8.8e-07	2.5	0.089	6.7e-11
SEG-GTEx × Coding (0.17%)	0.62	0.15	4.3e-05	22	3.2	4.6e-05
PPI-enhancer × ABC (0.58%)	1.2	0.21	3.5e-09	18	2	1.2e-07
PPI-enhancer × TSS (0.33%)	0.38	0.1	0.00017	19	1.8	3.6e-06
PPI-enhancer × Coding (0.24%)	0.38	0.097	7.2e-05	18	1.9	1.3e-05
PPI-enhancer × ATAC (0.41%)	0.6	0.17	0.00038	14	2.6	8.8e-07
ABC-G × TSS (0.38%)	0.34	0.12	0.0054	19	1.8	2.9e-06
EDS-binary × Roadmap (1.15%)	0.066	0.082	0.42	7.1	0.9	2.5e-05
SEG-GTEx × ABC (0.40%)	0.17	0.15	0.26	16	1.8	2.4e-06

Table S15. S-LDSC results for SNP annotations corresponding to the Weighted Enhancer gene score conditional on the baseline-LD+ model: Standardized Effect sizes ($\tau^\star$) and Enrichment (E) of 10 SNP annotations corresponding to the Weighted Enhancer gene score. The analysis is conditional on 93 baseline-LD+ annotations. Reports are meta-analyzed across 11 blood-related traits.

Annotation	$\tau^\star$	se($\tau^\star$)	p($\tau^\star$)	E	se(E)	p(E)
ABC (0.58%)	1	0.13	3.2e-14	17	1.3	8.2e-08
TSS (0.36%)	0.91	0.11	6.8e-16	22	1.7	1.1e-06
Coding (0.25%)	0.98	0.1	1.4e-20	23	2	1.5e-06
ATAC (0.44%)	0.64	0.15	2.2e-05	14	2.3	1.5e-07
eQTL (0.44%)	0.29	0.057	3.7e-07	8.6	0.9	2.8e-06
Roadmap (1.31%)	0.81	0.12	3.3e-11	12	1.1	4.3e-11
Promoter (0.64%)	0.86	0.087	4.4e-23	14	1.1	7.1e-07
PC-HiC (9.26%)	0.17	0.044	0.0001	3.1	0.17	1e-10
5kb (6.22%)	0.15	0.025	2.2e-09	3.4	0.14	2.1e-10
100kb (16.8%)	0.23	0.023	2.3e-23	2.8	0.088	1.2e-10

Table S16. S-LDSC results for SNP annotations corresponding to the Weighted Enhancer gene score conditional on the PPI-enhancer-driven joint model: Standardized Effect sizes ($\tau^\star$) and Enrichment (E) of SNP annotations corresponding to the Weighted Enhancer gene score. The analysis is conditional on 93 baseline-LD+ annotations and 7 annotations from the PPI-enhancer-driven joint model in Table S14. Reports are meta-analyzed across 11 blood-related traits.

Annotation	$\tau^\star$	se($\tau^\star$)	p($\tau^\star$)	E	se(E)	p(E)
ABC (0.58%)	-0.11	0.18	0.54	14	1.3	1.1e-06
TSS (0.36%)	0.2	0.14	0.13	19	1.7	8.7e-06
Coding (0.25%)	0.092	0.15	0.55	17	1.9	3.7e-05
ATAC (0.44%)	-0.083	0.083	0.32	11	2.1	2.6e-05
eQTL (0.44%)	0.11	0.055	0.04	7.1	0.89	1.8e-05
Roadmap (1.31%)	0.25	0.083	0.0021	9	0.97	7.3e-10
Promoter (0.64%)	0.23	0.092	0.014	11	1	1.8e-05
PC-HiC (9.26%)	0.014	0.033	0.68	2.9	0.16	1.4e-10
5kb (6.22%)	-0.036	0.028	0.2	3.5	0.14	2.8e-10
100kb (16.8%)	0.051	0.028	0.075	2.8	0.089	1.2e-10

Table S17. S-LDSC results for SNP annotations corresponding to the PPI-control gene score conditional on the baseline-LD+ model: Standardized Effect sizes ($\tau^\star$) and Enrichment (E) of 10 SNP annotations corresponding to the PPI-control gene score, conditional on 93 baseline-LD+ annotations. Reports are meta-analyzed across 11 blood-related traits.

	PPI-control-4					
	$\tau^\star$	se($\tau^\star$)	p($\tau^\star$)	E	se(E)	p(E)
ABC (0.46%)	0.59	0.13	3e-06	16	1.4	7.9e-07
TSS (0.25%)	0.6	0.11	1.3e-08	21	2	6.4e-06
Coding (0.23%)	0.39	0.093	3.2e-05	13	1.8	0.00024
ATAC (0.24%)	0.25	0.077	0.0013	9.6	1.6	0.00013
eQTL (0.31%)	0.17	0.043	5e-05	6.9	0.78	2.8e-05
Roadmap (0.49%)	0.32	0.075	2.3e-05	12	0.97	6.4e-07
Promoter (0.59%)	0.44	0.069	1.2e-10	8.7	0.88	2.7e-05
PC-HiC (7.55%)	0.098	0.033	0.0027	2.7	0.098	6.5e-08
5kb (5.86%)	0.089	0.018	8.2e-07	2	0.073	3.8e-07
100kb (16.7%)	0.11	0.018	6.8e-09	2	0.058	9e-09

Table S18. S-LDSC results for SNP annotations corresponding to the PPI-control gene score conditional on the PPI-enhancer-driven joint model: Standardized Effect sizes ($\tau^\star$) and Enrichment (E) of 10 SNP annotations corresponding to the PPI-control gene score, conditional on the PPI-enhancer-driven joint model from Table S14. Reports are meta-analyzed across 11 blood-related traits.

	PPI-control-4					
	$\tau^\star$	se($\tau^\star$)	p($\tau^\star$)	E	se(E)	p(E)
ABC (0.46%)	0.27	0.16	0.1	15	1.4	1.3e-06
TSS (0.25%)	0.27	0.11	0.014	18	1.9	2.2e-05
Coding (0.23%)	0.015	0.14	0.92	10	2	0.0032
ATAC (0.24%)	0.05	0.072	0.49	8.3	1.8	0.00049
eQTL (0.31%)	0.076	0.045	0.087	5.8	0.88	0.00019
Roadmap (0.49%)	0.25	0.077	0.0014	10	1	4.3e-06
Promoter (0.59%)	0.14	0.07	0.039	7	0.87	0.0002
PC-HiC (7.55%)	0.09	0.033	0.0071	2.7	0.1	3.1e-08
5kb (5.86%)	0.024	0.02	0.23	2.1	0.092	6.5e-07
100kb (16.7%)	0.07	0.027	0.01	2.1	0.071	3.2e-09

Table S19. S-LDSC results for SNP annotations corresponding to the RegNet-Enhancer gene score conditional on the baseline-LD+ model: Standardized Effect sizes ($\tau^\star$) and Enrichment (E) of SNP annotations corresponding to the RegNet-Enhancer gene score. The analysis is conditional on 93 baseline-LD+ annotations. Reports are meta-analyzed across 11 blood-related traits.

Annotation	$\tau^\star$	se($\tau^\star$)	p($\tau^\star$)	E	se(E)	p(E)
ABC (0.57%)	1.3	0.23	5.9e-09	19	2.2	3e-08
TSS (0.36%)	0.9	0.15	1.9e-09	23	2.5	4.6e-08
Coding (0.26%)	0.97	0.15	1e-10	21	2.4	5.2e-07
ATAC (0.36%)	0.79	0.17	4.8e-06	17	2.7	8.1e-08
eQTL (0.39%)	0.23	0.05	4.7e-06	8.1	0.76	3.5e-06
Roadmap (1.10%)	0.8	0.18	5.3e-06	13	1.5	3.9e-11
Promoter (0.68%)	0.73	0.087	4e-17	12	0.98	2.5e-07
PC-HiC (9.49%)	0.33	0.05	1.8e-11	3.4	0.17	8.6e-11
5kb (6.63%)	0.16	0.023	2e-11	3.1	0.11	4.1e-10
100kb (18.0%)	0.22	0.025	1.8e-19	2.6	0.083	6.9e-11

Table S20. S-LDSC results for SNP annotations corresponding to the RegNet-Enhancer gene score conditional on the PPI-enhancer-driven joint model: Standardized Effect sizes ($\tau^\star$) and Enrichment (E) of SNP annotations corresponding to the RegNet-Enhancer gene score. The analysis is conditional on 93 baseline-LD+ annotations and 7 annotations from the PPI-enhancer-driven joint model in Table S14. Reports are meta-analyzed across 11 blood-related traits.

Annotation	$\tau^\star$	se($\tau^\star$)	p($\tau^\star$)	E	se(E)	p(E)
ABC (0.57%)	0.53	0.19	0.0049	17	2	2.1e-07
TSS (0.36%)	0.38	0.15	0.009	20	2.4	2.6e-07
Coding (0.26%)	0.43	0.14	0.0023	16	1.9	6.1e-06
ATAC (0.36%)	0.38	0.14	0.0068	14	2.5	3.1e-06
eQTL (0.39%)	0.11	0.047	0.021	7	0.76	1.7e-05
Roadmap (1.10%)	0.47	0.16	0.0037	11	1.3	8.6e-10
Promoter (0.68%)	0.32	0.093	0.00057	10	0.95	1.3e-06
PC-HiC (9.49%)	0.23	0.05	3.6e-06	3.0	0.18	6.8e-09
5kb (6.63%)	0.063	0.023	0.0075	3.2	0.1	3.5e-10
100kb (18.0%)	0.12	0.042	0.042	2.3	0.077	5.1e-11

Table S21. S-LDSC results for Trans-Master and Transcription Factor (TF) SNP annotations conditional on the baseline-LD+cis model: Standardized Effect sizes ($\tau^\star$) and Enrichment (E) of 20 SNP annotations corresponding to Trans-Master and Transcription Factor genes. The analysis is conditional on 113 baseline-LD+cis model annotations. Reports are meta-analyzed across 11 blood-related traits.

Trans-Master

Annotation	$\tau^\star$	se($\tau^\star$)	p($\tau^\star$)	E	se(E)	p(E)
ABC (0.33%)	1.5	0.25	8e-10	32	2.5	8e-07
TSS (0.27%)	1.6	0.25	2.2e-10	44	3.3	5.7e-07
Coding (0.22%)	1.6	0.28	1.2e-08	32	4.9	1.8e-05
ATAC (0.21%)	0.9	0.17	6.4e-08	24	3.7	2.1e-06
eQTL (0.54%)	0.58	0.1	5.2e-09	11	1.5	1.7e-06
Roadmap (0.58%)	1.3	0.12	1.3e-25	22	1.4	3.6e-08
Promoter (0.57%)	1.1	0.18	1.9e-09	21	2.2	1.7e-06
PC-HiC (5.1%)	0.48	0.043	1.1e-29	5	0.18	5.3e-09
5kb (4.2%)	0.39	0.053	1.3e-13	5.3	0.29	1.9e-08
100kb (9.7%)	0.37	0.046	3.1e-16	3.8	0.17	8.7e-09

TF

Annotation	$\tau^\star$	se($\tau^\star$)	p($\tau^\star$)	E	se(E)	p(E)
ABC (0.32%)	0.48	0.13	0.00022	17	1.6	1.2e-06
TSS (0.16%)	0.88	0.18	1.2e-06	30	4.3	8.2e-07
Coding (0.16%)	0.32	0.086	0.00022	12	1.8	8.1e-05
ATAC (0.14%)	0.68	0.11	1.8e-10	23	3.1	8.3e-07
eQTL (0.17%)	0.03	0.037	0.41	4.1	0.87	0.0009
Roadmap (0.30%)	0.8	0.12	8.6e-12	21	2.3	1.1e-07
Promoter (0.37%)	0.31	0.08	0.00012	9.1	1.1	9e-05
PC-HiC (4.9%)	0.22	0.037	2.5e-09	3.3	0.14	1.5e-08
5kb (3.4%)	0.19	0.031	2.9e-10	2.8	0.16	2.7e-08
100kb (10.6%)	0.16	0.027	1.5e-09	2.3	0.055	1.2e-08

Table S22. Standardized Enrichment S-LDSC results for SNP annotations generated from Trans-master and Transcription Factor gene scores conditional on the baseline-LD+cis model.: Standardized Enrichment (StdE) of 20 SNP annotations corresponding to Trans-master and Transcription Factor genes. The analysis is conditional on the 113 baseline-LD+cis (93 baseline-LD+ and 10 Cis1 and 10 Cis3LD) annotations. Reports are meta-analyzed across 11 blood-related traits.

Trans-master

Annotation	*StdE*	se(*StdE*)	p(*StdE*)
ABC (0.33%)	1.8	0.14	8e-07
TSS (0.27%)	2.3	0.17	5.7e-07
Coding (0.22%)	1.5	0.23	1.8e-05
ATAC (0.21%)	1.1	0.17	2.1e-06
eQTL (0.54%)	0.8	0.11	1.7e-06
Roadmap (0.58%)	1.7	0.11	3.6e-08
Promoter (0.57%)	1.6	0.16	1.7e-06
PC-HiC (5.1%)	1.1	0.039	5.3e-09
5kb (4.2%)	1.1	0.059	1.9e-08
100kb (9.7%)	1.1	0.049	8.7e-09

TF

	StdE	se(*StdE*)	p(*StdE*)
ABC (0.32%)	0.97	0.09	1.2e-06
TSS (0.16%)	1.2	0.18	8.2e-07
Coding (0.16%)	0.49	0.073	8.1e-05
ATAC (0.14%)	0.84	0.11	8.3e-07
eQTL (0.17%)	0.17	0.035	0.0099
Roadmap (0.30%)	1.2	0.13	1.1e-07
Promoter (0.37%)	0.55	0.067	9e-05
PC-HiC (4.9%)	0.71	0.029	1.5e-08
5kb (3.4%)	0.51	0.028	2.7e-08
100kb (10.6%)	0.68	0.017	1.2e-08

Table S23. S-LDSC results for Trans-master and Transcription Factor (TF) SNP annotations conditional on the baseline-LD+ model: Standardized Effect sizes ($\tau^\star$) and Enrichment (E) of 20 SNP annotations corresponding to Trans-master and Transcription Factor genes. The analysis is conditional on 93 baseline-LD+ annotations. Reports are meta-analyzed across 11 blood-related traits.

Trans-master

Annotation	$\tau^\star$	se($\tau^\star$)	p($\tau^\star$)	E	se(E)	p(E)
ABC (0.33%)	2.3	0.17	3.5e-44	42	2.6	6.8e-08
TSS (0.27%)	2.6	0.23	6.4e-30	55	4	6.9e-08
Coding (0.22%)	2.4	0.28	2e-18	52	6	1.8e-07
ATAC (0.21%)	1.4	0.18	1.6e-14	33	4	1.3e-07
eQTL (0.54%)	0.9	0.11	3.4e-16	14	1.7	1.2e-07
Roadmap (0.58%)	1.7	0.11	2.1e-52	27	1.5	7.8e-09
Promoter (0.57%)	1.8	0.18	4.7e-22	27	2.4	8.4e-08
PC-HiC (5.1%)	0.69	0.041	3.9e-62	5.3	0.18	4.2e-09
5kb (4.2%)	0.59	0.049	1.1e-32	5.2	0.3	1.3e-08
100kb (9.7%)	0.56	0.044	2.5e-38	3.8	0.17	5.4e-09

TF

Annotation	$\tau^\star$	se($\tau^\star$)	p($\tau^\star$)	E	se(E)	p(E)
ABC (0.32%)	0.51	0.13	5.1e-05	17	1.7	2.5e-06
TSS (0.16%)	0.88	0.19	2.5e-06	30	4.4	8.6e-07
Coding (0.16%)	0.33	0.093	0.0004	12	1.9	0.00011
ATAC (0.14%)	0.7	0.11	1e-10	24	3.2	8.7e-07
eQTL (0.17%)	0.0086	0.039	0.83	4.5	0.9	0.0062
Roadmap (0.30%)	0.86	0.12	8.3e-13	23	2.4	4.1e-08
Promoter (0.37%)	0.34	0.084	6e-05	8.8	1.2	0.00018
PC-HiC (4.9%)	0.25	0.038	5.5e-11	3.3	0.14	1.2e-08
5kb (3.4%)	0.19	0.031	1.4e-09	2.8	0.16	3.2e-08
100kb (10.6%)	0.18	0.027	9.7e-11	2.2	0.058	8.3e-09

Table S24. S-LDSC results for Trans-master SNP annotations conditional on the baseline-LD+Cis1 model: Standardized Effect sizes ($\tau^\star$) and Enrichment (E) of 10 Trans-master SNP annotations conditional on 103 baseline-LD+Cis1 (93 baseline-LD+ and 10 Cis1) annotations where Cis1 represents S2G annotations linked to genes with at least 1 trait-associated cis-eQTL. Reports are meta-analyzed across 11 blood-related traits.

Trans-master						
Annotation	$\tau^\star$	se($\tau^\star$)	p($\tau^\star$)	E	se(E)	p(E)
ABC (0.33%)	1.9	0.18	1.5e-26	37	2.7	5.5e-07
TSS (0.27%)	1.8	0.22	7.8e-17	48	4.1	6.5e-07
Coding (0.22%)	1.8	0.29	2e-09	41	6	3.5e-06
ATAC (0.21%)	0.95	0.12	1e-15	27	3.6	1.4e-06
eQTL (0.54%)	0.7	0.12	3.4e-09	12	1.8	4.5e-07
Roadmap (0.58%)	1.4	0.12	1.8e-31	25	1.5	2.7e-08
Promoter (0.57%)	1.3	0.18	2.4e-13	24	2.8	7.2e-07
PC-HiC (5.1%)	0.51	0.041	4.1e-35	5	0.17	4.7e-09
5kb (4.2%)	0.45	0.05	2.8e-19	5.8	0.31	1.5e-08
100kb (9.7%)	0.41	0.046	8.3e-19	4	0.19	1.1e-08

Table S25. S-LDSC results for Trans-master SNP annotations conditional on the baseline-LD+Cis1+Cis2LD model: Standardized Effect sizes ($\tau^\star$) and Enrichment (E) of 10 Trans-master SNP annotations conditional on 113 baseline-LD+Cis1+Cis2LD (93 baseline-LD+ and 10 Cis1 and 10 Cis2LD) annotations where Cis1 represents S2G annotations linked to genes with at least 1 trait-associated cis-eQTL and Cis2LD represents S2G lined to genes with 2 unlinked trait-associated cis-eQTLs. Reports are meta-analyzed across 11 blood-related traits.

Trans-master

Annotation	$\tau^\star$	se($\tau^\star$)	p($\tau^\star$)	E	se(E)	p(E)
ABC (0.33%)	1.7	0.2	2.4e-16	32	2.4	5.6e-07
TSS (0.27%)	1.8	0.22	8.3e-16	45	3.5	5e-07
Coding (0.22%)	1.7	0.27	1.6e-10	34	4.9	9.7e-06
ATAC (0.21%)	1	0.17	1.1e-09	24	3.6	1.1e-06
eQTL (0.54%)	0.66	0.1	6.1e-11	11	1.5	9.2e-07
Roadmap (0.58%)	1.3	0.12	2e-28	22	1.4	2.4e-08
Promoter (0.57%)	1.2	0.17	9e-13	21	2.2	1.1e-06
PC-HiC (5.1%)	0.48	0.04	2e-32	5	0.17	5.3e-09
5kb (4.2%)	0.4	0.053	1.5e-14	5.3	0.3	1.6e-08
100kb (9.7%)	0.39	0.045	1.4e-17	3.8	0.17	7.5e-09

Table S26. S-LDSC results for Trans-master SNP annotations conditional on the baseline-LD+Cis1+Cis2 model: Standardized Effect sizes ($\tau^\star$) and Enrichment (E) of 10 Trans-master SNP annotations conditional on 113 baseline-LD+Cis1+Cis2 (93 baseline-LD+ and 10 Cis1 and 10 Cis2) annotations where Cis1 represents S2G annotations linked to genes with at least 1 trait-associated cis-eQTL and Cis2 represents S2G lined to genes with 2 not LD-corrected trait-associated cis-eQTLs. Reports are meta-analyzed across 11 blood-related traits.

Trans-master

Annotation	$\tau^\star$	se($\tau^\star$)	p($\tau^\star$)	E	se(E)	p(E)
ABC (0.33%)	1.5	0.21	6.7e-13	33	2.6	1.7e-06
TSS (0.27%)	1.3	0.3	5.8e-06	33	6	5e-05
Coding (0.22%)	1.3	0.3	5.8e-06	33	6	5e-05
ATAC (0.21%)	0.74	0.12	3.8e-10	23	3.4	5.3e-06
eQTL (0.54%)	0.57	0.12	1.3e-06	11	1.8	1.4e-06
Roadmap (0.58%)	1.1	0.12	4.1e-21	23	1.5	4.2e-08
Promoter (0.57%)	1	0.18	3.5e-08	21	3	2.6e-06
PC-HiC (5.1%)	0.4	0.04	3.1e-24	4.9	0.16	6.8e-09
5kb (4.2%)	0.34	0.056	1e-09	5.8	0.33	1.8e-08
100kb (9.7%)	0.31	0.053	5.5e-09	4	0.19	1.1e-08

Table S27. S-LDSC results for Trans-master SNP annotations conditional on the baseline-LD+Cis1+Cis3 model: Standardized Effect sizes ($\tau^\star$) and Enrichment (E) of 10 Trans-master SNP annotations conditional on 113 baseline-LD+Cis1+Cis3 (93 baseline-LD+ and 10 Cis1 + 10 Cis3) annotations where Cis1 represents S2G annotations linked to genes with at least 1 trait-associated cis-eQTL and Cis3 represents S2G lined to genes with 3 not LD-corrected trait-associated cis-eQTLs. Reports are meta-analyzed across 11 blood-related traits.

Trans-master

Annotation	$\tau^\star$	se($\tau^\star$)	p($\tau^\star$)	E	se(E)	p(E)
ABC (0.33%)	1.2	0.25	1.5e-06	29	2.4	2.4e-06
TSS (0.27%)	1.8	0.22	8.3e-16	45	3.5	5e-07
Coding (0.22%)	1.1	0.29	6.7e-05	26	5.2	0.00029
ATAC (0.21%)	1	0.17	1.1e-09	24	3.6	1.1e-06
eQTL (0.54%)	0.47	0.1	2.1e-06	10	1.5	3.4e-06
Roadmap (0.58%)	0.99	0.12	3.1e-16	21	1.4	3.8e-08
Promoter (0.57%)	0.8	0.19	1.8e-05	19	2.4	5.6e-06
PC-HiC (5.1%)	0.39	0.041	1.2e-20	4.9	0.16	8.2e-09
5kb (4.2%)	0.27	0.062	1.5e-05	5.4	0.32	1.8e-08
100kb (9.7%)	0.26	0.055	3e-06	3.9	0.17	7.5e-09

Table S28. S-LDSC results for Trans-master SNP annotations conditional on the baseline-LD+Cis1+Cis4 model: Standardized Effect sizes ($\tau^\star$) and Enrichment (E) of 10 Trans-master SNP annotations conditional on 113 baseline-LD+Cis1+Cis4 (93 baseline-LD+ and 10 Cis1 + 10 Cis4) annotations where Cis1 represents S2G annotations linked to genes with at least 1 trait-associated cis-eQTL and Cis4 represents S2G lined to genes with 4 not LD-corrected trait-associated cis-eQTLs. Reports are meta-analyzed across 11 blood-related traits.

Trans-master

Annotation	$\tau^\star$	se($\tau^\star$)	p($\tau^\star$)	E	se(E)	p(E)
ABC (0.33%)	1	0.28	0.00021	28	2.4	2.9e-06
TSS (0.27%)	1.1	0.27	4.4e-05	37	3.5	9.2e-06
Coding (0.22%)	0.88	0.29	0.0028	25	5.1	0.00032
ATAC (0.21%)	0.59	0.13	5.1e-06	19	3.3	1.4e-05
eQTL (0.54%)	0.38	0.11	0.00034	9.9	1.5	4.3e-06
Roadmap (0.58%)	0.86	0.12	1.7e-12	21	1.4	5.1e-08
Promoter (0.57%)	0.63	0.2	0.0012	18	2.4	1.7e-05
PC-HiC (5.1%)	0.36	0.044	6.2e-16	4.9	0.16	8.4e-09
5kb (4.2%)	0.24	0.063	0.0002	5.4	0.31	2.2e-08
100kb (9.7%)	0.23	0.058	7.3e-05	3.9	0.17	7.7e-09

Table S29. S-LDSC results for Trans-master SNP annotations conditional on the baseline-LD+cis model, but with all trait-associated trans-eQTLs removed.: Standardized Effect sizes ($\tau^\star$) and Enrichment (E) of 10 Trans-master SNP annotations, but with SNPs that are among the 3,853 trait-associated trans-eQTL SNPs that were used to construct the Trans-master gene score. The analysis is conditional on 113 baseline-LD+cis annotations. Reports are meta-analyzed across 11 blood-related traits.

	Trans-master					
Annotation	$\tau^\star$	se($\tau^\star$)	p($\tau^\star$)	E	se(E)	p(E)
ABC (0.33%)	1	0.21	1.8e-06	30	2.5	2.2e-06
TSS (0.27%)	0.85	0.28	0.002	39	4.1	2.7e-06
Coding (0.22%)	0.99	0.29	0.00051	29	5.7	0.00012
ATAC (0.21%)	0.56	0.13	2.3e-05	19	3.2	2e-05
eQTL (0.54%)	0.43	0.12	0.00023	10	1.8	5.1e-06
Roadmap (0.58%)	0.98	0.11	2.4e-19	21	1.5	9.6e-08
Promoter (0.57%)	0.8	0.18	1.2e-05	20	2.7	4.9e-06
PC-HiC (5.1%)	0.41	0.04	2.7e-24	4.7	0.16	6.5e-09
5kb (4.2%)	0.34	0.049	4.7e-12	5.4	0.29	3.8e-08
100kb (9.7%)	0.32	0.046	5.2e-12	3.9	0.18	1.8e-08

Table S30. S-LDSC results for jointly significant Trans-master and Transcription Factor SNP annotations: Standardized Effect sizes ($\tau^\star$) and Enrichment (E) of SNP annotations that are significant in a joint analysis of all marginally significant Trans-master and Transcription Factor (TF) SNP annotations. The analysis is conditional on 113 baseline-LD+cis annotations. Reports are meta-analyzed across 11 blood-related traits.

Annotation	$\tau^\star$	se($\tau^\star$)	p($\tau^\star$)	E	se(E)	p(E)
Trans-master × Roadmap (0.58%)	0.81	0.13	5.4e-10	19	1.4	8.4e-08
Trans-master × PC-HiC (5.1%)	0.2	0.044	8.3e-06	4.6	0.16	5.9e-09
Trans-master × 5kb (4.2%)	0.19	0.049	1.1e-04	5.2	0.29	2.3e-08
TF × ATAC (0.14%)	0.4	0.08	7.2e-07	17	2.5	7e-06
TF × Roadmap (0.30%)	0.58	0.11	2.2e-07	19	2.2	2.7e-07

Table S31. S-LDSC results for Trans-regulated SNP annotations conditional on the baseline-LD+cis model: Standardized Effect sizes ($\tau^\star$) and Enrichment (E) of 10 SNP annotations corresponding to Trans-regulated genes. The analysis is conditional on 113 baseline-LD+cis annotations. Reports are meta-analyzed across 11 blood-related traits.

Trans-Regulated						
Annotation	$\tau^\star$	se($\tau^\star$)	p($\tau^\star$)	E	se(E)	p(E)
ABC (0.87%)	-0.12	0.15	0.43	10	0.97	1.1e-06
TSS (0.70%)	0.068	0.11	0.54	14	1.3	2.1e-05
Coding (0.56%)	0.2	0.095	0.04	9.3	1.3	0.0004
ATAC (0.72%)	0.12	0.077	0.13	7.5	1.1	9.2e-06
eQTL (1.07%)	0.016	0.049	0.74	4	0.54	0.00028
Roadmap (1.67%)	-0.091	0.11	0.41	7.8	0.75	2.2e-08
Promoter (1.47%)	0.02	0.072	0.78	6.1	0.6	0.00012
PC-HiC (16.0%)	-0.057	0.044	0.2	2.4	0.075	3.2e-09
5kb (14.9%)	-0.021	0.02	0.3	2.2	0.046	4.9e-09
100kb (34.7%)	-0.023	0.019	0.23	1.9	0.044	1.8e-09

Table S32. S-LDSC results for Trans-regulated SNP annotations conditional on the baseline-LD+ model: Standardized Effect sizes ($\tau^\star$) and Enrichment (E) of 10 SNP annotations corresponding to Trans-regulated genes. The analysis is conditional on 93 baseline-LD+ annotations. Reports are meta-analyzed across 11 blood-related traits.

Trans-Regulated						
Annotation	$\tau^\star$	se($\tau^\star$)	p($\tau^\star$)	E	se(E)	p(E)
ABC (0.87%)	0.37	0.16	0.018	11	0.98	4.2e-07
TSS (0.70%)	0.5	0.11	5.6e-06	15	1.2	9.1e-06
Coding (0.56%)	0.55	0.098	2.3e-08	12	1.2	6.4e-05
ATAC (0.72%)	0.34	0.099	0.00053	8.2	1.1	1.5e-06
eQTL (1.07%)	0.091	0.051	0.075	4.8	0.53	2.9e-05
Roadmap (1.67%)	0.23	0.1	0.028	8.6	0.76	4.6e-09
Promoter (1.47%)	0.38	0.072	8e-08	6.7	0.57	5.7e-05
PC-HiC (16.0%)	0.033	0.04	0.4	2.4	0.076	2.6e-09
5kb (14.9%)	0.033	0.02	0.1	2.2	0.049	2.6e-09
100kb (34.7%)	0.016	0.019	0.41	1.9	0.042	8.4e-10

Table S33. S-LDSC results restricted to 6 autoimmune traits for Trans-master SNP annotations conditional on baseline-LD+cis model: Standardized Effect sizes ($\tau^\star$) and Enrichment (E) of 10 Trans-master SNP annotations conditional on 113 baseline-LD+cis annotations, with results meta-analyzed across 5 Autoimmune traits.

	Trans-master					
Annotation	$\tau^\star$	se($\tau^\star$)	p($\tau^\star$)	E	se(E)	p(E)
ABC (0.33%)	0.89	0.33	0.0069	28	4	0.0002
TSS (0.27%)	1	0.27	0.00016	37	5.4	8.5e-05
Coding (0.22%)	0.91	0.3	0.0024	20	6	0.0053
ATAC (0.21%)	0.81	0.29	0.0052	25	6.4	0.0006
eQTL (0.54%)	0.37	0.11	0.00067	7.6	1.6	0.00031
Roadmap (0.58%)	1.1	0.18	1.3e-09	23	2.3	4.5e-05
Promoter (0.57%)	0.66	0.18	0.00037	16	2.2	0.00031
PC-HiC (5.1%)	0.41	0.075	5.8e-08	5.2	0.32	9.4e-06
5kb (4.2%)	0.27	0.054	6.5e-07	4.8	0.41	7.4e-06
100kb (9.7%)	0.25	0.047	8.6e-08	3.5	0.22	5.5e-06

Table S34. S-LDSC results for SNP annotations corresponding to the PPI-master gene score conditional on the baseline-LD+cis model: Standardized Effect sizes ($\tau^\star$) and Enrichment (E) of 10 SNP annotations corresponding to the PPI-master gene score, conditional on 113 baseline-LD+cis annotations. Reports are meta-analyzed across 11 blood-related traits.

	PPI-Master					
	$\tau^\star$	se($\tau^\star$)	p($\tau^\star$)	E	se(E)	p(E)
ABC (0.44%)	1.6	0.17	5.1e-21	27	1.9	9.8e-08
TSS (0.30%)	1.7	0.16	5.6e-27	41	2.8	2.1e-07
Coding (0.23%)	1.7	0.14	4.2e-33	37	2.8	1.2e-06
ATAC (0.25%)	1.3	0.17	4.6e-15	29	3.3	7.6e-09
eQTL (0.37%)	0.47	0.058	2.5e-16	12	1.1	2.4e-06
Roadmap (0.60%)	1.5	0.12	4.4e-33	25	1.9	5.5e-09
Promoter (0.59%)	1.1	0.11	4.3e-26	21	1.4	8e-07
PC-HiC (7.09%)	0.38	0.05	2.5e-14	4	0.12	5.8e-09
5kb (4.80%)	0.38	0.031	2.4e-35	4.6	0.13	8.6e-09
100kb (14.3%)	0.37	0.028	1.1e-40	3.2	0.075	4.7e-09

Table S35. Standardized enrichment of SNP annotations corresponding to PPI-master gene score conditional on the baseline-LD+cis model: Standardized enrichment of the 10 SNP annotations corresponding to the PPI-master gene score, conditional on 113 baseline-LD+cis annotations respectively. Reports are meta-analyzed across 11 blood-related traits.

	PPI-master		
	$StdE$	se($StdE$)	p($StdE$)
ABC (0.44%)	1.8	0.12	9.8e-08
TSS (0.30%)	2.2	0.15	2.1e-07
Coding (0.23%)	1.8	0.13	1.2e-06
ATAC (0.25%)	1.5	0.17	7.6e-09
eQTL (0.37%)	0.72	0.069	2.4e-06
Roadmap (0.60%)	1.9	0.15	5.5e-09
Promoter (0.59%)	1.6	0.11	8e-07
PC-HiC (7.09%)	1	0.031	5.8e-09
5kb (4.80%)	0.98	0.028	8.6e-09
100kb (14.3%)	1.1	0.026	4.7e-09

Table S36. S-LDSC results for SNP annotations corresponding to the PPI-master gene score conditional on the baseline-LD+ model: Standardized Effect sizes ($\tau^\star$) and Enrichment (E) of 10 SNP annotations corresponding to the PPI-master gene score, conditional on 93 baseline-LD+ annotations. Reports are meta-analyzed across 11 blood-related traits.

	PPI-Master					
	$\tau^\star$	se($\tau^\star$)	p($\tau^\star$)	E	se(E)	p(E)
ABC (0.44%)	2.2	0.15	1.5e-47	33	1.9	1.8e-08
TSS (0.30%)	2.5	0.16	3e-55	50	2.8	4.2e-08
Coding (0.23%)	2.4	0.14	3.3e-61	50	2.9	5e-08
ATAC (0.25%)	1.7	0.19	5.7e-20	34	3.4	1.1e-09
eQTL (0.37%)	0.77	0.061	3.4e-36	15	1.2	2.2e-07
Roadmap (0.60%)	1.8	0.11	9.2e-64	28	1.8	2e-09
Promoter (0.59%)	1.7	0.11	6.7e-51	25	1.4	8.4e-08
PC-HiC (7.09%)	0.56	0.038	2.8e-47	4.2	0.12	3.4e-09
5kb (4.80%)	0.51	0.029	3e-68	4.6	0.13	5.5e-09
100kb (14.3%)	0.52	0.025	3.9e-93	3.2	0.073	2.6e-09

Table S37. S-LDSC results for SNP annotations corresponding to the PPI-master gene score conditional on the Master-regulator joint model: Standardized Effect sizes ($\tau^\star$) and Enrichment (E) of 10 SNP annotations corresponding to the PPI-master gene score, conditional on the Master-regulator joint model from Table S30. Reports are meta-analyzed across 11 blood-related traits.

	PPI-master					
	$\tau^\star$	se($\tau^\star$)	p($\tau^\star$)	E	se(E)	p(E)
ABC (0.44%)	0.8	0.14	1.8e-08	21	1.8	7.7e-07
TSS (0.30%)	0.85	0.16	5e-08	30	2.7	2.9e-06
Coding (0.23%)	0.84	0.13	9.5e-11	23	2.7	4.4e-05
ATAC (0.25%)	0.73	0.15	1.5e-06	23	3	6e-08
eQTL (0.37%)	0.23	0.057	6.5e-05	9.3	0.99	1.5e-05
Roadmap (0.60%)	0.9	0.12	5.9e-15	23	1.8	9.6e-09
Promoter (0.59%)	0.49	0.11	3.9e-06	15	1.5	1.6e-05
PC-HiC (7.09%)	0.15	0.051	0.003	3.8	0.11	8.3e-09
5kb (4.80%)	0.2	0.028	2e-12	4.6	0.13	7.8e-09
100kb (14.3%)	0.18	0.024	6.7e-15	3.2	0.072	4.9e-09

Table S38. S-LDSC results for a joint analysis of all SNP annotations corresponding to the master-regulator and PPI-master gene scores. Standardized Effect sizes ($\tau^\star$) and Enrichment (E) of the significant SNP annotations in a joint analysis comprising of marginally significant Master-regulator SNP annotations from Figure 4B and PPI-master SNP annotations. Reported are the results for the jointly significant annotations only. Also marked in red are annotations that are jointly Bonferroni significant in the Master-regulator joint model in Figure S6 but not Bonferroni significant in this model. All analyses are conditional on 113 baseline-LD+cis annotations. Results are meta-analyzed across 11 blood-related traits.

Annotation	$\tau^\star$	se($\tau^\star$)	p($\tau^\star$)	E	se (E)	p(E)
Trans-master × Roadmap (0.58%)	0.50	0.14	0.0003	21	1.4	5.1e-08
Trans-master × PCHiC (5.1%)	0.24	0.049	1.2e-06	4.7	0.17	7.5e-09
PPI-master × Coding (0.23%)	0.54	0.13	2.4e-05	19	2.7	0.00067
PPI-master × ATAC (0.25%)	0.63	0.14	7.4e-06	20	2.9	1.7e-07
PPI-master × Roadmap (0.60%)	0.93	0.14	2.8e-11	23	1.8	1.5e-08
Trans-master× 5kb (4.2%)	0.34	0.12	0.0054	19	1.8	2.9e-06
TF × ATAC (0.14%)	0.066	0.082	0.42	7.1	0.9	2.5e-05
TF × Roadmap (0.30%)	0.17	0.15	0.26	16	1.8	2.4e-06

Table S39. S-LDSC results for the combined joint analysis of SNP annotations corresponding to Enhancer-driven, PPI-enhancer, Master-regulator and PPI-master gene scores conditional on the baseline-LD+cis model. Standardized Effect sizes ($\tau^\star$) and Enrichment (E) of the significant SNP annotations in a combined joint model comprising of marginally significant Enhancer-driven, PPI-enhancer, Master-regulator and PPI-master SNP annotations. All analysis are conditional on 113 baseline-LD+cis annotations. Results are meta-analyzed across 11 blood-related traits.

Annotation	$\tau^\star$	se($\tau^\star$)	p($\tau^\star$)	E	se (E)	p(E)
ATAC-distal × Promoter (1.8%)	0.25	0.07	0.0003	6.4	0.53	2.3e-05
EDS-binary × 100kb (14.6%)	0.077	0.019	4.3e-05	2.5	0.088	1.4e-10
PPI-enhancer × ABC (0.58%)	0.99	0.23	1.2e-05	18	2.2	6.7e-08
PPI-enhancer × Coding (0.24%)	0.57	0.13	1.3e-05	17	2.2	9.1e-06
Trans-master × Roadmap (0.58%)	0.51	0.14	0.0003	20	1.4	7.1e-08
Trans-master × PC-HiC (5.1%)	0.25	0.049	2.5e-07	4.8	0.17	6.6e-09
PPI-master × ATAC (0.25%)	0.61	0.13	2.3e-06	20	2.7	2e-07
PPI-master × Roadmap (0.60%)	0.91	0.12	7.1e-14	22	1.5	2.3e-08

Table S40. Combined $\tau^\star$ of various joint models. We report combined $\tau^\star$ scores (as well as standard errors, t statistic and p-value) for the several joint models studied.

	CDS	se(CDS)	pvalue
Master-regulator (joint; Table S30)	1.5	0.15	4.7e-24
Enhancer (joint; Table S42)	1.3	0.17	9.6e-16
Master-regulator + PPI-master (joint; Table S38)	1.9	0.14	1.1e-40
Enhancer + PPI-enhancer (joint; Table S41)	1.5	0.15	4.7e-24
Enhancer +Master-regulator+ PPI-enhancer + PPI-master (joint; Table S39)	2.5	0.24	1.1e-25
Enhancer+Master-regulator+PPI-enhancer + PPI-master +pLI (joint; Table S45)	2.7	0.25	1e-26
Enhancer+Master-regulator+PPI-enhancer + PPI-master +PPI-all (joint; Table S46)	2.5	0.22	4.4e-29

Table S41. S-LDSC results for a joint analysis of SNP annotations corresponding to Enhancer-driven and PPI-enhancer gene scores conditional on baseline-LD+cis model. Standardized Effect sizes ($\tau^\star$) and Enrichment (E) of the significant SNP annotations in the PPI-enhancer-driven joint model in Table S14 conditional on 113 baseline-LD+cis annotations. Results are meta-analyzed across 11 blood-related traits.

ATAC-distal × Promoter (1.8%)	0.28	0.071	6.3e-05	6.5	0.54	3e-05
EDS-binary × 100kb (14.6%)	0.091	0.02	3.1e-06	2.5	0.087	1.1e-10
SEG-GTEx × Coding (0.17%)	0.4	0.16	0.01	19	3.4	0.00024
PPI-enhancer × ABC (0.58%)	0.86	0.2	1e-05	17	2	2.3e-07
PPI-enhancer × TSS (0.33%)	0.32	0.1	0.0015	19	1.7	3.1e-06
PPI-enhancer × Coding (0.24%)	0.37	0.093	5.8e-05	17	1.9	1.7e-05
PPI-enhancer × ATAC (0.41%)	0.51	0.16	0.0018	14	2.5	3.5e-06

Table S42. S-LDSC results for a joint analysis of all SNP annotations corresponding to Enhancer-driven gene scores conditional on baseline-LD+cis model. Standardized Effect sizes ($\tau^\star$) and Enrichment (E) of the significant SNP annotations in the Enhancer driven joint model in Table S8 conditional on 113 baseline-LD+cis annotations. Results are meta-analyzed across 11 blood-related traits.

Annotation	$\tau^\star$	se($\tau^\star$)	p($\tau^\star$)	E	se (E)	p(E)
ABC-G × TSS (0.38%)	0.4	0.11	0.00021	17	1.7	4.5e-06
ATAC-distal × Promoter (1.84%)	0.29	0.071	3.2e-05	6.7	0.54	2.3e-05
EDS-binary × Roadmap (1.15%)	0.28	0.093	0.003	8.4	0.88	5e-09
EDS-binary × 100kb (14.6%)	0.088	0.02	1.1e-05	2.5	0.087	1.2e-10
SEG-GTEx × ABC (0.40%)	0.33	0.13	0.011	16	1.7	2.7e-06
SEG-GTEx × Coding (0.17%)	0.5	0.16	0.0016	18	3.4	0.00034

Table S43. $\Delta\log l_{SS}$ results for the different heritability models. We report $\Delta\log l_{SS}$ derived from the $\log l_{\mathrm{SS}}$ metric, proposed in ref.[56], for the different heritability models studied in this paper: baseline-LD, baseline-LD+, baseline-LD+Enhancer (86 baseline-LD annotations and the 6 jointly significant annotations from Figure S5), baseline-LD+PPI-enhancer (86 baseline-LD annotations and 7 jointly significant annotations from Figure 3D), baseline-LD+cis, baseline-LD+master (113 baseline-LD+cis and 4 jointly significant annotations from Figure S6), baseline-LD+PPI-master (113 baseline-LD+cis and 4 jointly significant annotations from Figure 4D) and baseline-LD+final (113 baseline-LD+cis and 8 jointly significant annotations from Figure 5). We compute $\Delta\log l_{SS}$ as the difference in $\log l_{\mathrm{SS}}$ for each model with respect to s baselineLD-no-funct model with 17 annotations that include no functional annotations[56,90]. We also report the percentage increase in $\Delta\log l_{SS}$ for each model over the baseline-LD model. We do not report AIC as the number of annotations are not too different to alter conclusions based on just the $\log l_{\mathrm{SS}}$. We report three summary $\log l_{\mathrm{SS}}$ results - one averaged across 30 UK Biobank traits[90] (All), one averaged across 6 blood-related traits from UK Biobank (Blood) and one averaged across the other 24 non blood related traits from UK Biobank (Non-blood) (Table S44). Averaged across all traits, we observe a +22.4% improvement from the annotations of the final joint model (baseline-LD+final) over baseline-LD. Of this 22.4%, we observe a +5.1% larger improvement in this metric from the 7 new S2G annotations constituting baseline-LD+ and +13% larger improvement from the 7 new S2G, plus the 20 annotations in baseline-LD+cis model. The remainder of the improvement (22.4% - 13% = 9.4%) comes from the 8 jointly significant annotations in the final joint model in Figure 5. The percentage increase was higher for the non-blood-related traits case as the $\log l_{\mathrm{SS}}$ values, on average, were considerably smaller in comparison to the blood related traits.

Model	$\Delta\log l_{\mathrm{SS}}$ (All)	% incr. over baseline-LD (All)	pval (All)	$\Delta\log l_{\mathrm{SS}}$ (Blood)	% incr. over baseline-LD (Blood)	pval (Blood)	$\Delta\log l_{\mathrm{SS}}$ (Non-blood)	% incr. over baseline-LD (Non-blood)	pval (Non-blood)
baseline-LD (n=86)	1379	0	-	2668	0	-	1121	0	-
baseline-LD+ (n=93)	1449	5.1%	5e-27	2879	7.8%	1e-86	1163	3.7%	3e-115
baseline-LD+ Enhancer (n=99)	1507	9.3%	3e-47	3081	15%	5e-186	1193	6.3%	8e-24
baseline-LD+ PPI-enhancer (n=100)	1537	11.4%	5e-59	3208	20%	1e-220	1202	7.2%	2e-27
baseline-LD+cis (n=113)	1564	13.4%	6e-62	2532	-5.0%	1.00	1370	22.2%	3e-88
baseline-LD+ Master (n=117)	1669	21%	2e-102	2952	10.6%	1e-99	1412	25.9%	1e-102
baseline-LD+ PPI-master (n=117)	1681	21.8%	2e-107	2986	11.9%	9e-114	1419	26.6%	9e-106
baseline-LD+final (n=121)	1688	22.4%	9e-108	2998	12.3%	3e-116	1425	27.2%	9e-106

Table S44. List of UKBiobank traits used for logl_{SS} calculations. The list consists of 6 blood-related traits and 24 non blood-related traits.

Trait	Category	N
disease AID Sure	Blood	459324
blood Eosinophil count	Blood	439938
Blood Platelet count	Blood	444382
Blood Red count	Blood	445174
Blood RBC distr. width	Blood	442700
blood White count	Blood	444502
reproduction Menarche Age	Non-blood	242278
reproduction Menopause Age	Non-blood	143025
Body balding	Non-blood	208336
Body BMIz	Non-blood	457824
cov EDU Years	Non-blood	454813
disease Dermatology	Non-blood	459324
disease Allergy Eczema	Non-blood	458699
lung FVCzSmoke	Non-blood	371949
lung FEV1FVCzSmoke	Non-blood	371949
pigment Hair	Non-blood	452720
bmd Heel Tscorez	Non-blood	445921
body Heightz	Non-blood	458303
disease Hi-chol-self-rep	Non-blood	459324
disease Hypothyroidism self rep	Non-blood	459324
Other Morning-person	Non-blood	41050
Mental Neuroticism	Non-blood	372066
disease Respiratory ENT	Non-blood	459324
pigment Skin	Non-blood	453609
cov Smoking Status	Non-blood	457683
pigment Sunburn	Non-blood	344229
bp SystolicadjMedz	Non-blood	422771
pigment Tanning	Non-blood	449984
disease T2D	Non-blood	459324
body WHRadjBMIz	Non-blood	458417

Table S45. S-LDSC results for the combined joint model of all SNP annotations corresponding to Enhancer-driven, PPI-enhancer, Master-regulator, PPI-master and pLI gene scores conditional on baseline-LD+cis model. Standardized Effect sizes ($\tau^\star$) and Enrichment (E) of the significant SNP annotations in a joint model comprising of Enhancer-driven, PPI-enhancer, Master-regulator, PPI-master and pLI SNP annotations. All analysis are conditional on 113 baseline-LD+cis annotations. Results are meta-analyzed across 11 blood-related traits.

Annotation	$\tau^\star$	se($\tau^\star$)	p($\tau^\star$)	E	se (E)	p(E)
ATAC-distal × Promoter (1.8%)	0.25	0.07	0.0003	6.5	0.53	2e-05
EDS-binary × 100kb (14.6%)	0.071	0.019	0.00014	2.5	0.088	1.4e-10
PPI-enhancer × ABC (0.58%)	0.93	0.22	2.2e-05	17	2.2	7.4e-08
PPI-enhancer × Coding (0.24%)	0.56	0.13	1.7e-05	17	2.2	9e-06
Trans-master × Roadmap (0.58%)	0.54	0.14	0.00015	20	1.3	7.5e-08
Trans-master × PC-HiC (5.1%)	0.25	0.049	2.7e-07	4.8	0.17	6.7e-09
PPI-master × ATAC (0.25%)	0.64	0.13	1.5e-06	20	2.8	1.4e-07
PPI-master × Roadmap (0.60%)	0.79	0.12	3.3e-11	22	1.5	2.4e-08
pLI × Roadmap (1.19%)	0.53	0.085	5.5e-10	10	0.85	7e-09

Table S46. S-LDSC results for the combined joint model of all SNP annotations corresponding to Enhancer-driven, PPI-enhancer, Master-regulator, PPI-master and PPI-all gene scores conditional on baseline-LD+cis model. Standardized Effect sizes ($\tau^\star$) and Enrichment (E) of the significant SNP annotations in a joint model comprising of Enhancer-driven, PPI-enhancer, Master-regulator, PPI-master and PPI-all SNP annotations. All analysis are conditional on 113 baseline-LD+cis annotations. Results are meta-analyzed across 11 blood-related traits.

Annotation	$\tau^\star$	se($\tau^\star$)	p($\tau^\star$)	E	se (E)	p(E)
ATAC-distal × Promoter (1.8%)	0.26	0.069	0.00013	6.4	0.53	2.3e-05
EDS-binary × 100kb (14.6%)	0.087	0.019	2.5e-06	2.5	0.089	1.3e-10
Trans-master × Roadmap (0.58%)	0.56	0.14	3.4e-05	20	1.3	7.2e-08
Trans-master × PC-HiC (5.1%)	0.25	0.048	3.9e-07	4.7	0.17	5.9e-09
PPI-master × ATAC (0.25%)	0.56	0.13	8e-06	19	2.7	3.3e-07
PPI-master × Roadmap (0.60%)	0.58	0.13	4.6e-06	22	1.4	2.7e-08
PPI-all × ABC (0.53%)	0.7	0.15	1.7e-06	18	1.9	1.4e-07
PPI-all × Coding (0.23%)	0.56	0.1	5.2e-08	18	2.1	0.00012
PPI-all × Roadmap (0.81%)	0.7	0.18	7.9e-05	19	1.9	3.6e-10

Table S47. S-LDSC results for the less restrictive combined joint model of all SNP annotations corresponding to both Enhancer-driven, PPI-enhancer, Master-regulator and PPI-master gene scores conditional on the baseline-LD+ model. Standardized Effect sizes ($\tau^\star$) and Enrichment (E) of the significant SNP annotations in a joint model comprising of Enhancer-driven, PPI-enhancer, Master-regulator and PPI-master SNP annotations. All analysis are conditional on 113 baseline-LD+cis annotations. Results are meta-analyzed across 11 blood-related traits.

Annotation	$\tau^\star$	se($\tau^\star$)	p($\tau^\star$)	E	se (E)	p(E)
ATAC-distal × Promoter (1.8%)	0.42	0.07	2.5e-09	6.4	0.5	2e-05
EDS-binary × 100kb (14.6%)	0.084	0.019	1.3e-05	2.5	0.09	1e-10
SEG-GTEx × Coding (0.17%)	0.55	0.14	0.0003	20	3.3	7.6e-05
PPI-enhancer × ABC (0.58%)	1.3	0.24	1.2e-07	18	2.2	4.5e-08
PPI-enhancer × Coding (0.24%)	0.42	0.11	0.00022	17	2.2	6.1e-06
Trans-master × Roadmap (0.58%)	0.82	0.16	1.5e-07	22	1.3	3.2e-08
Trans-master × PC-HiC (5.1%)	0.34	0.037	1.7e-19	4.9	0.16	6.9e-09
PPI-master × ATAC (0.25%)	0.69	0.14	4.1e-07	20	2.7	1.1e-07
PPI-master × Roadmap (0.60%)	0.93	0.12	3.2e-14	23	1.3	1.3e-08

Table S48. MAGMA gene-set analysis p-values for all gene scores, meta-analysed across blood-related traits: Meta-analysed p-value across 11 independent blood-related diseases and traits for binarized (taking top 10% if the actual gene score is probabilistic) Enhancer-driven, Master-regulator, PPI-enhancer and PPI-master gene scores in a MAGMA competitive gene sets analysis.

Gene Score	p-value
ABC-G	4.4e-10
ATAC-distal	3.7e-04
EDS-binary	2.5e-49
eQTL-CTS	5.6e-06
Expecto-MVP	0.015
PCHiC-distal	7.8e-100
SEG-GTEx	1.3e-12
Trans-master	3.1e-122
TF	1.8e-186
PPI-enhancer	2.5e-12
PPI-master	4.3e-110

2 Supplementary Figures

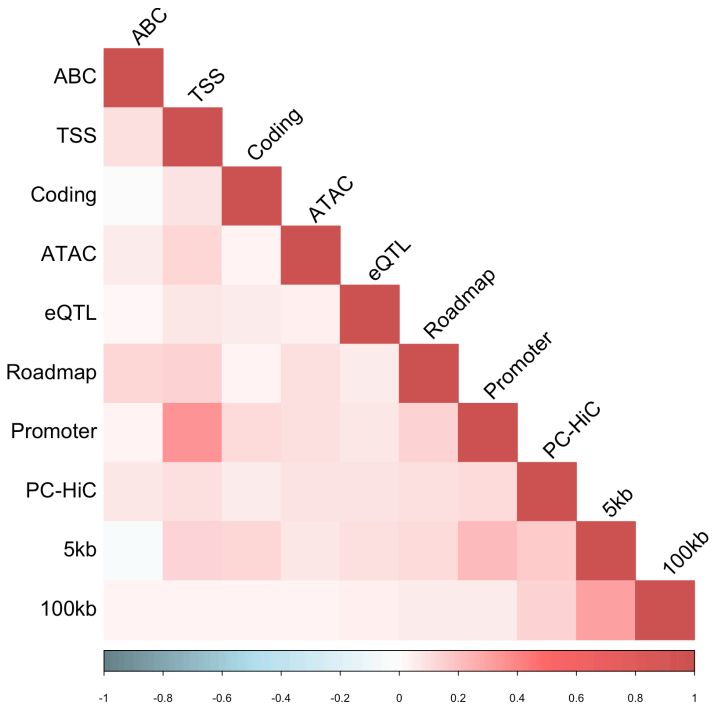

Figure S1. Correlation between SNP-to-gene (S2G) linking strategies. Correlation matrix of all 10 SNP-to-gene (S2G) linking strategies (Table 2), as assessed by the sets of SNPs linked to genes.

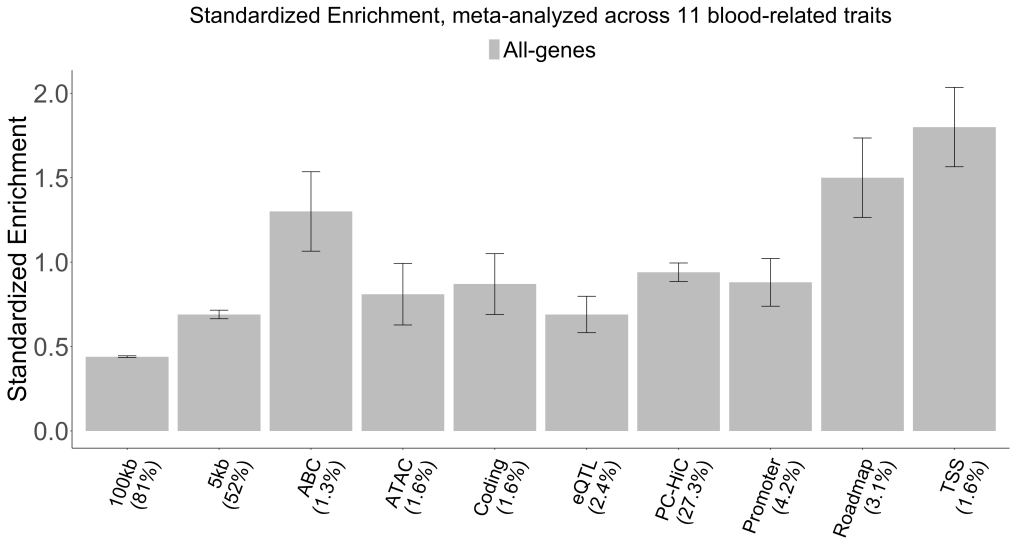

Figure S2. Standardized enrichment of SNP annotations for SNPs linked to all genes. Barplot representing standardized enrichment metric, as proposed in ref.[11] for 10 SNP annotations corresponding SNPs linked to all genes by 10 S2G strategies from Table 2.

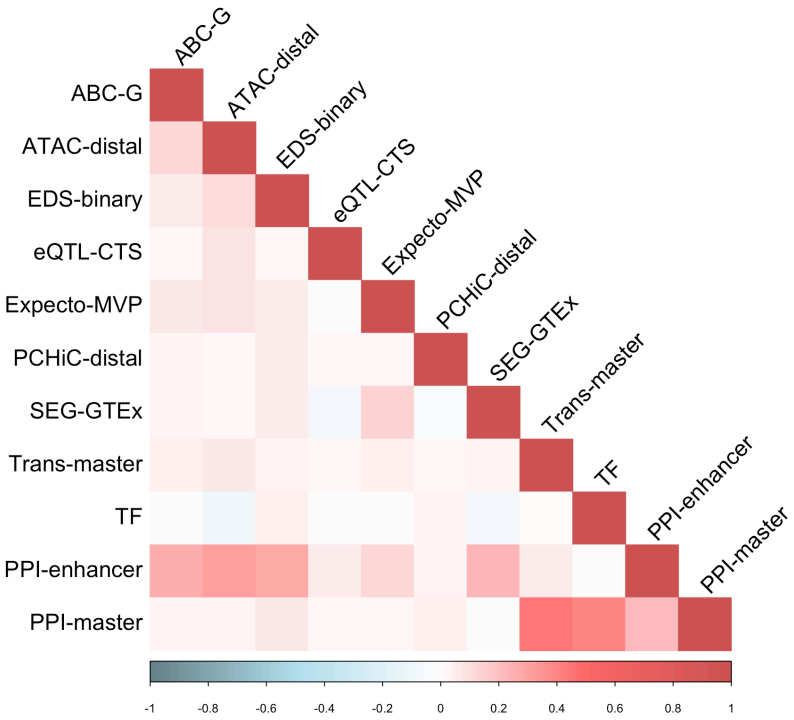

Figure S3. Correlation between different gene scores. Correlation matrix of all 11 gene scores (7 enhancer-driven, 2 master-regulator, 1 PPI-enhancer-driven and 1 PPI-master) from Table 1 across all genes.

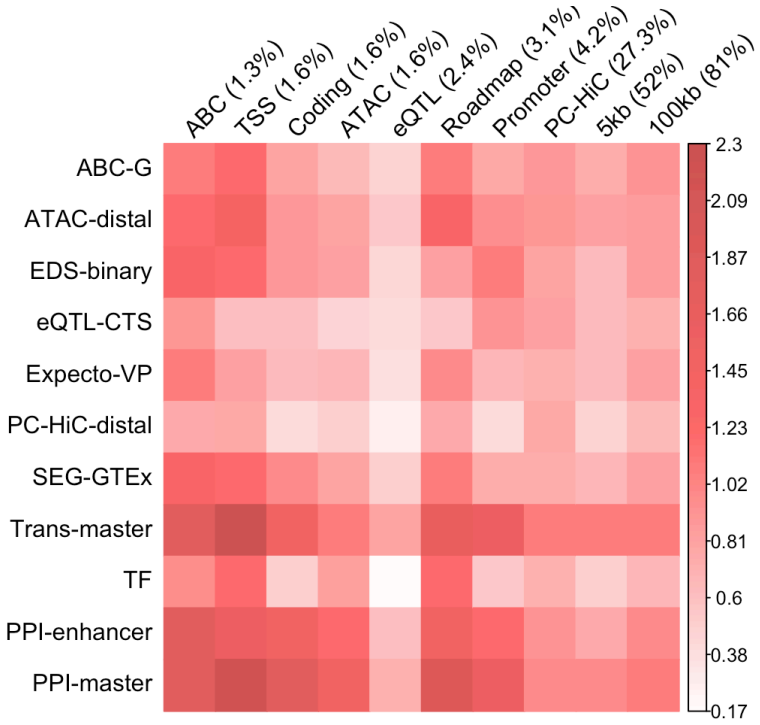

Figure S4. Standardized enrichment of SNP annotations corresponding to all gene scores. Heatmap representing standardized enrichment metric, as proposed in ref.[11] for all SNP annotations corresponding to all 11 gene scores (7 enhancer-driven, 2 master-regulator, 1 PPI-enhancer-driven and 1 PPI-master) stacked sequentially from top to bottom.

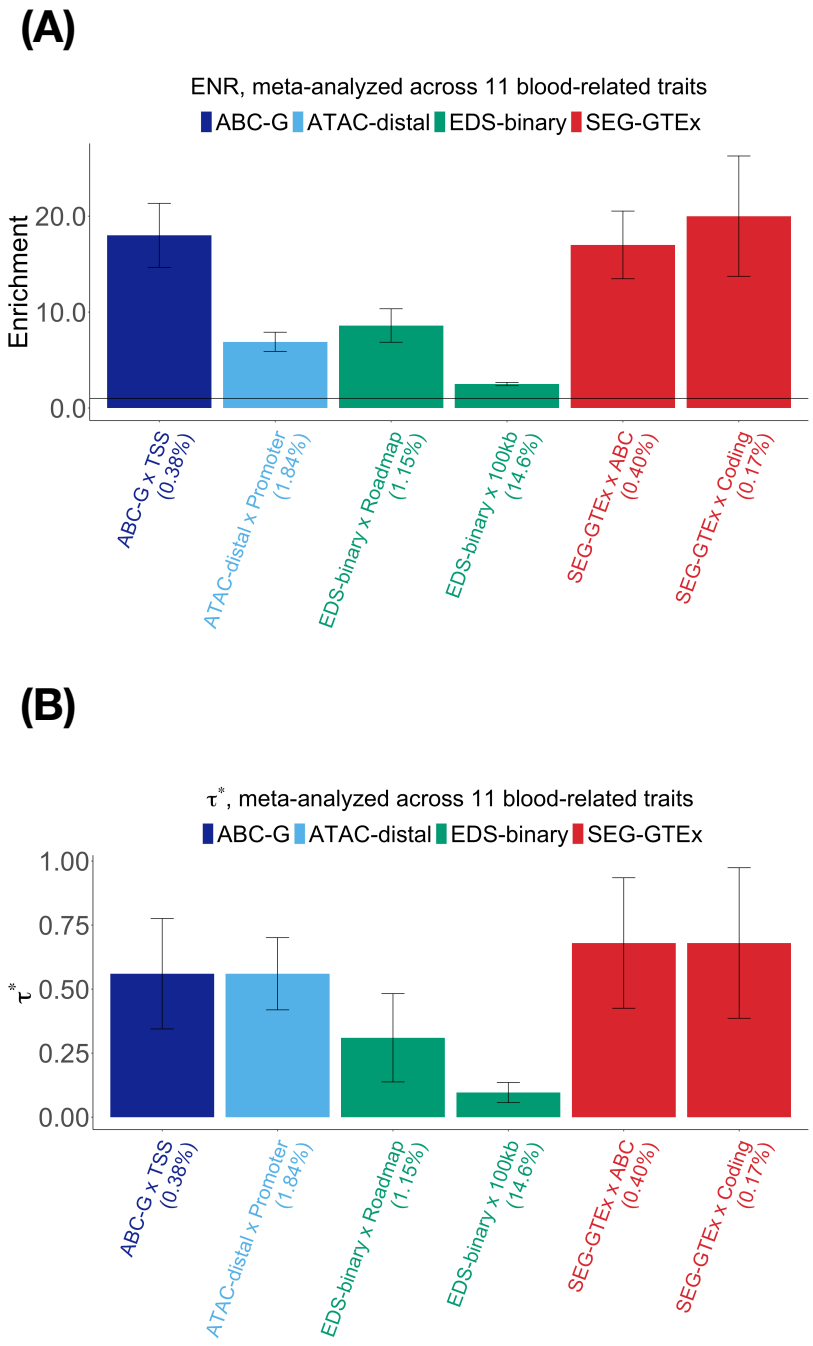

Figure S5. Disease informativeness of Enhancer-driven annotations in a joint analysis: (Panel A) Heritability enrichment, conditional on the Enhancer-driven joint model. Horizontal line denotes no enrichment. (Panel B) Standardized effect size $\tau^\star$ conditional on the same model. Results are shown only for the SNP annotations that are significant in the joint analysis after Bonferroni correction (0.05/110). Errors bars represent 95% confidence intervals. Numerical results are reported in Table S8.

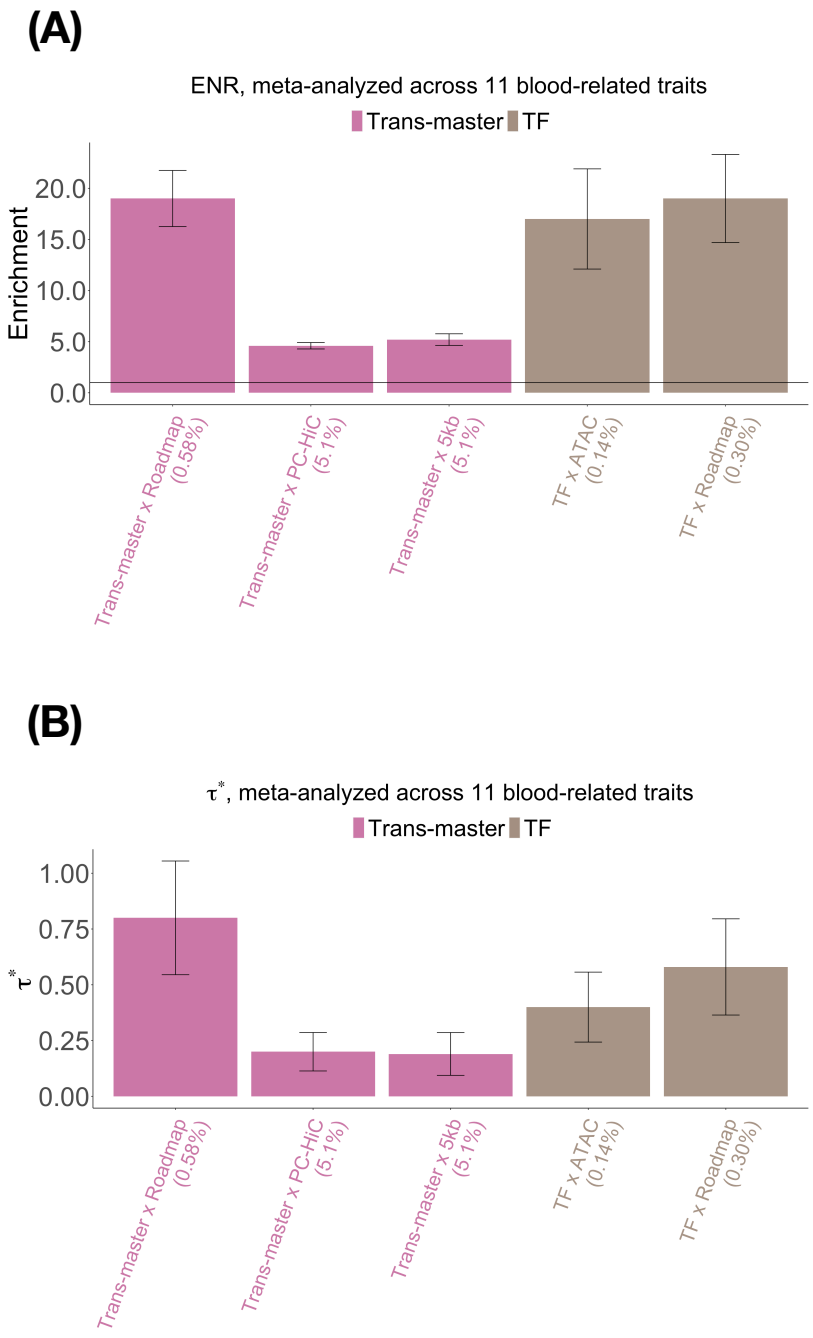

Figure S6. Disease informativeness of Master-regulator annotations in a joint analysis: (Panel A) Heritability enrichment, conditional on the Master-regulator joint model. Horizontal line denotes no enrichment. (Panel B) Standardized effect size $\tau^\star$ conditional on the same model. Results are shown only for the SNP annotations that are significant in the joint analysis after Bonferroni correction (0.05/110). Errors bars represent 95% confidence intervals. Numerical results are reported in Table S30.

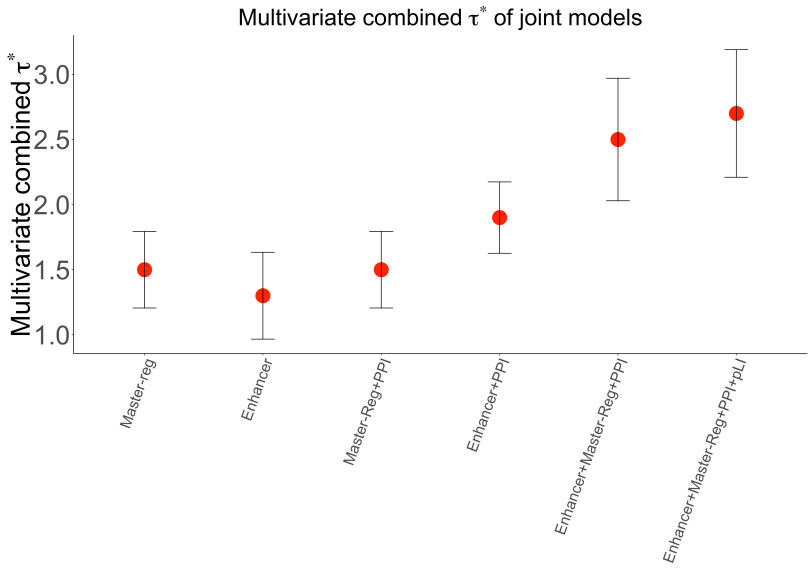

Figure S7. Combined $\tau^\star$ of different joint models studied: A plot of the combined $\tau^\star$ metric for different joint models. Numerical results are reported in Table S40.

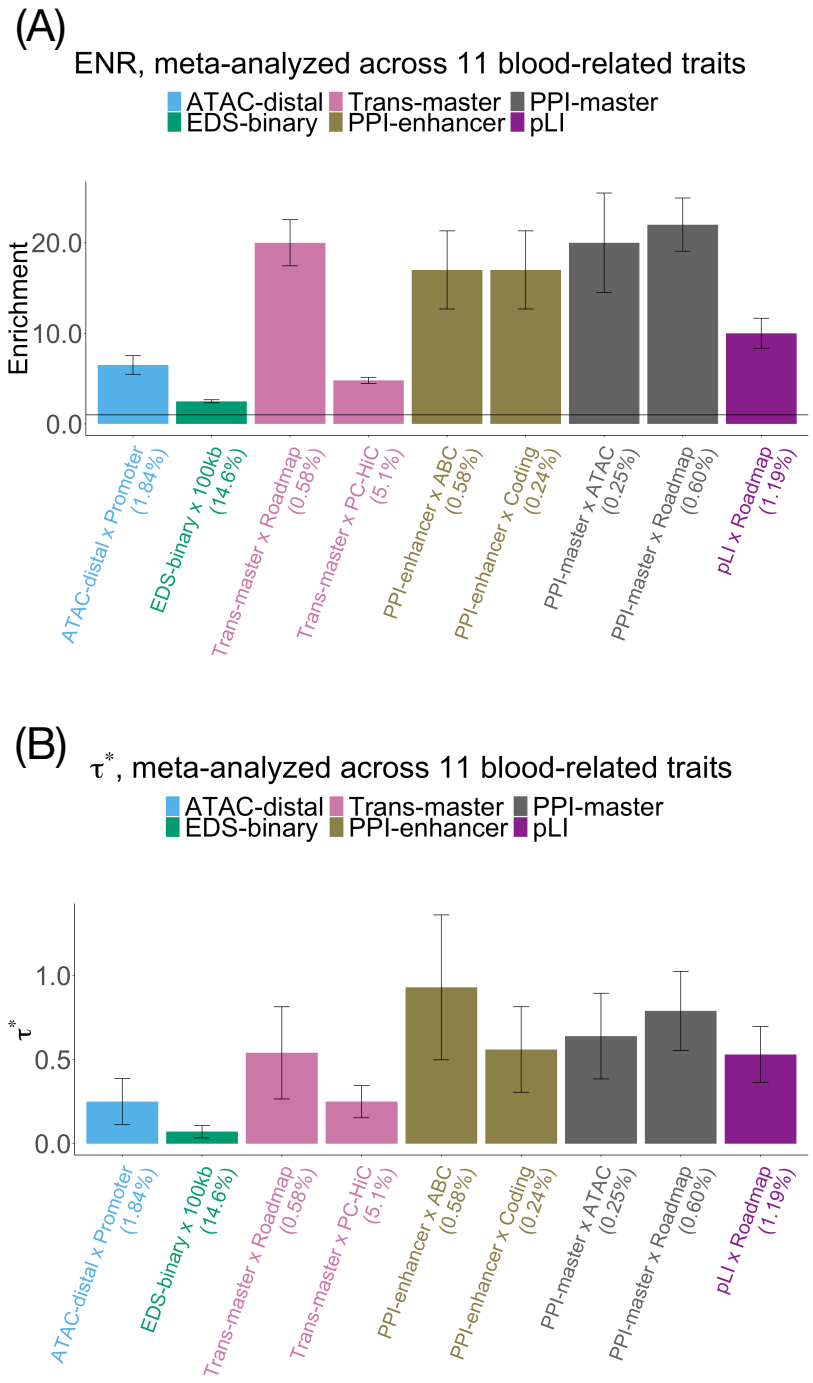

Figure S8. Disease informativeness of Enhancer-driven, PPI-enhancer, Master-regulator, PPI-master and pLI SNP annotations in a joint analysis: (Panel A) Heritability enrichment, conditional on the combined joint model of Enhancer-driven, PPI-enhancer, Master-regulator, PPI-master and pLI SNP annotations. Horizontal line denotes no enrichment. (Panel B) Standardized effect size $\tau^{\star}$ conditional on the same model. Results are shown only for the SNP annotations that are significant in the joint model after Bonferroni correction (0.05/110). Errors bars represent 95% confidence intervals. Numerical results are reported in Table S45.